The feasibility of using digital image processing and Fura-2 fluorescent dye to monitor changes in $[Ca^{2+}]_i$ in blood platelets

by

Samer Nabhan Karmi

A Thesis Submitted to the
Graduate Faculty in Partial Fulfillment of the
Requirements for the Degree of
MASTER OF SCIENCE

Interdepartmental Program: Biomedical Engineering
Major: Biomedical Engineering

Approved:

Iowa State University
Ames, Iowa

1989

TABLE OF CONTENTS

PAGE

CHAPTER ONE: INTRODUCTION

There is a plethora of theories in which calcium is postulated to have a critical signaling role in a wide variety of tissues. It is not surprising to see, after all, that the number of techniques for measuring intracellular free calcium concentrations exceeds those for measuring other ions such as potassium, sodium, chloride, and magnesium [Tsien, 1983].

In blood platelets, calcium is believed to be an important mediator linking responses such as shape change and aggregation to the stimulus evoking them such as ADP. Many reports have shown that $[Ca^{2+}]_i$ increased in ADP-stimulated platelets [Sage and Rink, 1986].

Fluorescence microscopy utilizing fluorescent labels to study cells or cell constituents has been used for many years. Recently, Fura-2, a fluorescent calcium-sensitive dye, was synthesized. Since then, a great deal of research utilizing this dye to measure $[Ca^{2+}]_i$ in a variety of cells, including platelets, has been forthcoming.

The purpose of this study is to determine the feasibility of using fluorescence microscopy and digital image processing to monitor changes in $[Ca^{2+}]_i$ in Fura-2-loaded canine platelets activated with the agonist ADP.

CHAPTER TWO: LITERATURE REVIEW

In this chapter, a brief description of the histology of platelets and their role in hemostasis and the role of calcium in platelet activation are outlined. A historical review of the optical indicators used to detect $[Ca^{2+}]$ is briefly given, and the properties of the Fura-2 fluorescent dye are detailed. Reports utilizing this dye to measure increasing $[Ca^{2+}]_i$ in platelets in response to the agonist ADP are mentioned. The advantages as well as the limitations of this probe are also discussed.

Platelets

Histology and function

Platelets are small, 2-4 μm in diameter, nonnucleated discs which are found circulating in relatively large numbers, typically 200,000-400,000 cells/μL, in the peripheral blood [Matthews, 1987; Yardumian et al., 1986]. Platelets function in hemostasis, help maintain vascular integrity, enhance coagulation, and participate in the inflammatory response [Jain, 1986]. The megakaryocytes, giant cells in the bone marrow, form platelets by pinching off bits of their cytoplasm and extruding them into the circulation.

Platelets contain a peripheral ring of microtubules, actin and myosin, glycogen, lysosomes, and two types of

granules: dense granules which secrete non-protein substances in response to platelet activation and α-granules which contain hormones that are thought to stimulate wound healing [Ganong, 1987]. Platelets also contain two unique groups of canaliculi: the surface connected or open canalicular system, and the dense tubular system (DTS), which is believed to be the calcium sequestering site [White and Gerrard, 1978].

Mammalian platelets respond to a variety of stimuli by changing their shape and then aggregating. The aggregation response is dependent upon the aggregating agent and its concentration and the origin of platelets [Meyers, 1985]. According to White and Gerrard [1978], "The loss of the discoid shape, development of an irregular, roughly spherical configuration with multiple spikey and bulky pseudopods, and movement of randomly disposed organelles into tightly packed masses in cell centers are among the most dramatic events in platelet response to aggregating agents." Canine platelets can be activated by mixing them with ADP prepared in buffered saline solution at a 10 μM concentration [Clemmons and Meyers, 1984]. The sequence of platelet activation is summarized in Table 2.1.

Table 2.1. Platelet function in haemostatic process

From Yardumian et al. [1986]

Damaged vessel wall

|

Platelet adhesion and plasma VIIIvWf[a] multimers interaction

|

Activation of platelet membrane receptors

|

Platelet shape change and aggregation

|

Platelet activation proceeds by: arachidonic acid metabolism; increase of free cytoplasmic calcium ions; release of platelet activating factor

|

Release of granule contents

|

Irreversible aggregate formed

|

Flip-flop of outer membrane promotes coagulation cascade

---

[a] Factor VIII von Willebrand factor.

The role of calcium in platelet activation

Calcium is very important in platelet activation [Yardumian et al. 1986]. The pathways of platelet activation are schematically shown in Figure 2.1. Much evidence points toward calcium as the intracellular mediator which links the interaction between the stimulus and the membrane to the observed response in platelets [Jones, 1985].

In resting platelets, free $[Ca^{2+}]_i$ generally ranges between 10 and 100 nM, and between 1 and 10 μM in response to external stimuli such as ADP [Jones, 1985; Hallam and Rink, 1985]. The elevation of $[Ca^{2+}]_i$ is believed to occur by recruitment of internal stores as well as influx from external media [Feinstein et al., 1985]. The extent of platelet activation is believed to be dependent on the ultimate $[Ca^{2+}]_i$; responses such as shape change and adhesion require low Ca^{2+} concentrations while secretion and irreversible aggregation require higher concentrations [Jones, 1985]. The calcium released from the dense tubular system binds with calmodulin and this coenzyme phosphorylates myosin thereby activating the actomyosin contractile system of filaments beneath the platelet membrane. It also initiates α-granules' and dense granules' contents release [Jones, 1985; Yardumian et al., 1986; Feinstein et al., 1985].

FIGURE 2.1. Schematic representation of pathways of platelet activation

Ca^{++} = calcium ion;

PGG_2, H_2, E_2, D_2 and $F_{2\alpha}$ = prostaglandins G_2, H_2, E_2, D_2, and $F_{2\alpha}$, respectively.

TXA_2 = thromboxane A_2;

TXB_2 = thromboxane B_2;

Beta-TG = Beta-thromboglobulin;

PF_4 = platelet factor 4;

FDGF = platelet derived growth factor;

ADP = adenosine diphosphate;

ATP = adenosine triphosphate.

From Yardumian et al. [1986]

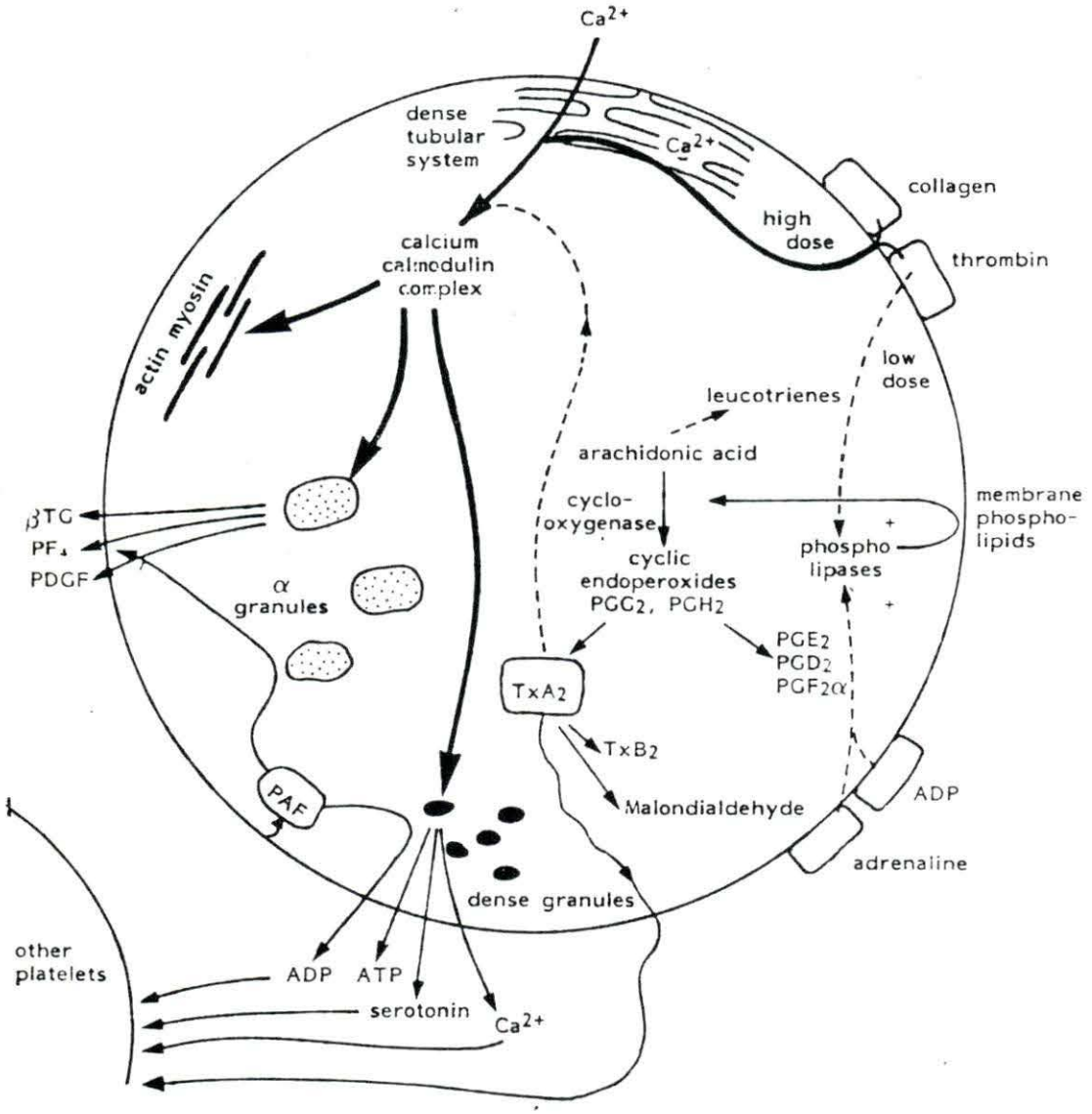
Ca2+
dense tubular system
Ca2+
collagen
high dose
thrombin
calcium calmodulin complex
actin myosin
low dose
leucotrienes
arachidonic acid
cyclo-oxygenase
membrane phospho-lipids
phospho lipases
βTG
PF4
PDGF
α granules
cyclic endoperoxides PGG2, PGH2
PGE2
PGD2
PGF2α
TxA2
TxB2
Malondialdehyde
PAF
ADP
adrenaline
dense granules
other platelets
ADP
ATP
serotonin
Ca2+

Detection and Measurement of $[Ca^{2+}]_i$

The ability to experimentally measure the cytoplasmic free calcium ion concentration in biological cells has provided evidence of the critical role this ion plays both as an internal messenger and as a regulator in cell physiology. Several methods, both electrical and optical, exist to measure and detect $[Ca^{2+}]_i$.

Optical indicators reviewed in this section fall into three categories: bioluminescent, metallochromic and fluorescent indicators. Bioluminescent and metallochromic indicators will be briefly outlined and more detailed analysis will be given for the tetracarboxylate dyes Quin-2/AM and Fura-2/AM which are members of the fluorescent indicator family.

Bioluminescent indicators

Aequorin and Obelin are photoproteins which are extracted from a number of marine organisms which exhibit bioluminescence [Blinks et al., 1982; Tsien, 1983]. They can be introduced into large cells by microinjection, microsecond high voltage pulses, and hypo-osmotic shock which breaks the plasma membrane permeability barrier [Tsien, 1983].

Calcium-activated photoproteins emit blue light at a rate that is highly sensitive to the free calcium ion concentration. Luminescence can be quantified by

measuring the intensity of the light emitted. This is done by a photomultiplier tube which is sensitive enough to detect low light intensities [Campbell et al., 1979]. However, these photoproteins do not bind calcium with 1:1 stoichiometry (which makes quantitative measurement of $[Ca^{2+}]_i$ very difficult), and they are very difficult to introduce into small cells because of their large molecular size [Blinks and Moore, 1986].

Metallochromic indicators

Metallochromic dyes are low molecular weight substances which undergo a color change upon binding metal ions such as calcium [Blinks et al., 1982]. Arsenazo III, Antipylarzo III, and Dichlorophosphonazo III are metallochromic dyes which are used as $[Ca^{2+}]_i$ indicators.

Studies have shown that these dyes do not bind to Ca^{2+} with a simple 1:1 stoichiometry and that they also bind to Mg^{2+} and H^{+}. This makes quantitative measurements of $[Ca^{2+}]_i$ very difficult if not impossible [Tsien, 1983; Blinks et al., 1982; Scarpa, 1979].

Fluorescent indicators

Fluorescent indicators emit light of characteristic spectral properties when illuminated with radiation in the wavelength range defined by the fluorescence excitation spectrum of the particular indicator [Blinks et al., 1982].

Interaction with calcium ions could result in a simple change in fluorescence intensity, a shift in emission spectrum, or a shift of excitation spectrum, any or all of which could be used to detect a change in the amount of Ca^{2+} bound to the indicator.

Fluorescent indicators such as Chlortetracycline, Calcein, and fluorescently labeled proteins have been used to detect $[Ca^{2+}]_i$ in a variety of <u>in vitro</u> preparations. Chlortetracycline was used to investigate $[Ca^{2+}]_i$ in human platelets [Le Breton et al., 1976; Feinstein, 1980]. However, Chlortetracycline does not detect $[Ca^{2+}]_i$ directly, but rather it detects membrane-bound high calcium, i.e., those areas of membrane which contain high concentrations of calcium [Blinks et al., 1982].

Another category of fluorescent indicators is the tetracarboxylate dyes of which Indo-1, Quin-2, and Fura-2 are members. It has been found that these dyes bind calcium with 1:1 stoichiometry [Grynkiewicz et al., 1985; Tsien et al., 1982].

Indo-1 shifts both its absorption and emission maxima to lower wavelengths when bound to calcium. This makes it suited for flow cytometry experiments [Tsien, 1986]. Properties and biological applications of this dye are reported, for example, by Grynkiewicz et al. [1985], Tsien [1986], Luckhoff [1986] and Bush and Jones [1987].

Quin-2 This dye was utilized by Hallam and Rink [1985] in measuring $[Ca^{2+}]_i$ changes in human platelets in response to the agonist ADP. The platelets were in suspension and measurements were obtained by spectrophotometry.

Several papers have reported platelet responses to different agonists in which Quin-2 was employed to measure changes in $[Ca^{2+}]_i$ [Hallam and Rink, 1985; Rao et al., 1985; Rink et al., 1982; Sage and Rink, 1986; Pollock and Rink, 1986]. Several shortcomings in the properties of Quin-2 were reported. (1) The dissociation constant K_d, defined as

$$K_d = \frac{[Ca^{2+}]\ [Dye]}{[Ca^{2+}\ Dye]}$$

[Tsien, 1983] of Quin-2 is 113 nM, which causes dye saturation at calcium concentrations above 1 μM. (2) Quin-2 fluoresces weakly because of its low quantum efficiency (0.029 and 0.14 for the free dye and Ca^{2+} dye complex, respectively) and its low extinction coefficient ($5 \times 10^3\ M^{-1}\ cm^{-1}$ for both free and calcium-bound dye) [Tsien, 1983]; therefore, intracellular concentrations between 0.3 and 1 mM are required to get a signal substantially in excess of background fluorescence [Rink and Pozzan, 1985]. (3) Quin-2 signals $[Ca^{2+}]$ only as a change in fluorescence intensity. Thus, factors such as illuminator intensity, emission collection efficiency,

dye concentration and effective cell thickness affect fluorescence emission signal; hence, Quin-2 fluorescence signals can be seriously misleading [Grynkiewicz et al., 1985]. (4) Quin-2 has relatively poor selectivity for Ca^{2+} over Mg^{2+} and divalent heavy metal cations. Thus, variations in $[Mg^{2+}]_i$, for example, would affect the calibration scale for the fluorescence signals [Grynkiewicz et al., 1985].

Fura-2 The following is a description of the properties which make Fura-2 a better fluorescent indicator than Quin-2 for measuring $[Ca^{2+}]_i$. The method of introducing the dye into cells, reports of utilizing Fura-2 to measure $[Ca^{2+}]_i$ in platelets and other cells, and some limitations of this probe are also presented.

The optical properties of Fura-2 in the presence and absence of Ca^{2+} are shown in Table 2.2 [Grynkiewicz et al., 1985]. Fura-2 absorbance maxima are near uv with extinction coefficients in the range of 3×10^4 M^{-1} cm^{-1}. The binding of Ca^{2+} shifts all the absorbance spectra to shorter wavelengths. Both calcium-free and calcium-bound Fura-2 fluoresce quite strongly with the quantum efficiency increasing from 0.23 for the free dye to 0.49 for the Ca^{2+} complex. The fluorescence excitation spectra shift to shorter wavelengths as the $[Ca^{2+}]$ increases much like absorbance spectra do; however, the binding of Ca^{2+}

Table 2.2. Optical Properties of Calcium-Free and Calcium-Bound Fura-2. Absorption maxima refer to the dominant peaks at longest wavelengths, measured in 100 mM KCl at 22 ± 2°C. Emission maxima peaks were measured on a Perkin Elmer MPF-44 spectrophotometer. Emission maxima and quantum efficiencies were measured in 100 mM KCl at 22 ± 2°C
From Grynkiewicz et al. [1985]

Apparent K_d for Ca^{2+} (nM)	135[a], 224[b]	
	Free Anion	Ca^{2+} Complex
Absorption maxima (nm)	362	335
Extinction Coefficient (1/M cm)	27×10^3	33×10^3
Emission Maxima (nm)	512	505
Fluorescence Quantum Efficiency	0.23	0.49

[a] In 100 mM KCl, 20°C, pH 7.1-7.2.

[b] In 115 mM KCl, 20 mM NaCl, 10mM-K-MOPS, pH 7.05, 1mM free Mg^{2+}, 37°C.

shifts the wavelengths of the emission maxima much less than it shifts the excitation maxima.

Binding of Ca^{2+} by Fura-2 enhances fluorescence emissions at 510 nm when excitation is at 340 nm, but reduces it when excitation is at 380 nm [Ashley et al., 1985]. The ability of Ca^{2+} to alter the wavelengths and the amplitudes of the fluorescence response of Fura-2 allows for calculating $[Ca^{2+}]_i$ by the ratio of fluorescence intensity at excitation wavelengths of 340 and 380 nm. This method is believed to eliminate possible variability due to instrument efficiency, dye concentration, and the cell thickness [Grynkiewicz et al., 1985; Connor et al., 1987]. This technique [Grynkiewicz et al., 1985] yields the following equation:

$$[Ca^{2+}] = K_d \left[\frac{R - R_{min}}{R_{max} - R} \right] \left[\frac{F_o}{F_s} \right] \quad , \quad \text{where}$$

R is the ratio of fluorescence intensity at 340 nm over that at 380 nm observed at unknown $[Ca^{2+}]$;

$\mathbf{R_{min}}$ is the intensity ratio at no ($< 10^{-8}$ nM) $[Ca^{2+}]$;

$\mathbf{R_{max}}$ is the intensity ratio at maximum (> 100 μM) $[Ca^{2+}]$;

$\mathbf{F_o/F_s}$ is the ratio of fluorescence intensity produced by 380 nm exciting radiation at low and saturated Ca^{2+} levels, respectively; and

$\mathbf{K_d}$ is the dissociation constant of the dye-calcium reaction.

Fura-2's relatively high affinity for Ca^{2+} is much lower than that of Quin-2; according to Tsien [1980] the relatively high affinity has two advantages. (1) It is desirable to have a dye with K_d values close to the resting $[Ca^{2+}]_i$ (typically 10^{-8}-10^{-7} M) because the dye would be very sensitive to variations at this level. (2) The high affinity for Ca^{2+} only requires dye-loading of small quantities for a given optical sensitivity, thereby reducing the toxic side effects and minimizing perturbations of cell function. Fura-2 has been found not only to be sensitive to changes in $[Ca^{2+}]$ around 10^{-8}-10^{-7} M, but it has also been reported that $[Ca^{2+}]$ of up to 15 μM has also been successfully measured [Al-Mohanna and Hallett, 1988].

Fura-2 has a lower affinity for Mg^{2+} (K_d = 5.6 mM) than for Ca^{2+}. Furthermore, the effect of Mg^{2+} binding on the Fura-2 spectrum is small in comparison to that of Ca^{2+} [Grynkiewicz et al., 1985]. It is found that both Fe^{2+} and Mn^{2+} quench Fura-2 because of their many unpaired electrons. Fura-2 prefers Ca^{2+} over Mn^{2+} by 510:1; however, Fe^{2+} binds Fura-2 between 3 and 10 times as strongly as does Ca^{2+} [Grynkiewicz et al., 1985].

Calcium-free and calcium-bound Fura-2 were found to be independent of pH excursions within physiological range [Grynkiewicz et al., 1985]. This is due to the largely

deprotonated nitrogen sites which bear the carboxylates [Rink and Pozzan, 1985].

Fura-2, a tetracarboxylic anion, seems not to cross or adhere to cell membranes significantly [Tsien et al., 1984]. However, when Fura-2 is esterified with acetoxymethyl tetraester, the esterified derivative (Fura-2/AM) is passively absorbed into the cell [Tsien, 1981]. Once inside the cell, Fura-2/AM is hydrolyzed by cytoplasmic esterases to Fura-2 as shown in Figure 2.2. The hydrolysis of acetoxymethyl tetraester yields acetic acid and formaldehyde, which is toxic; surprisingly, low toxicity has been reported with cells loaded with esterified dyes [Tsien et al., 1984].

Reports of experimental results on several types of cells have shown that Fura-2 is distributed throughout the cytosol and nucleus, but not into mitochondria, lysosomes, endoplasmic reticulum, or secretory granules [Rink and Pozzan, 1985; Al-Mohanna and Hallett, 1988]. In contrast, Almers and Neher [1985] suggest that Fura-2 accumulated to a significant degree in the secretory granules of rat mast cells.

Studies done on rat neutrophils indicate that Fura-2 leaked from cells at a very slow rate ($0.16 \pm 0.05\%\ min^{-1}$ at 37°C) [Al-Mohanna and Hallett, 1988].

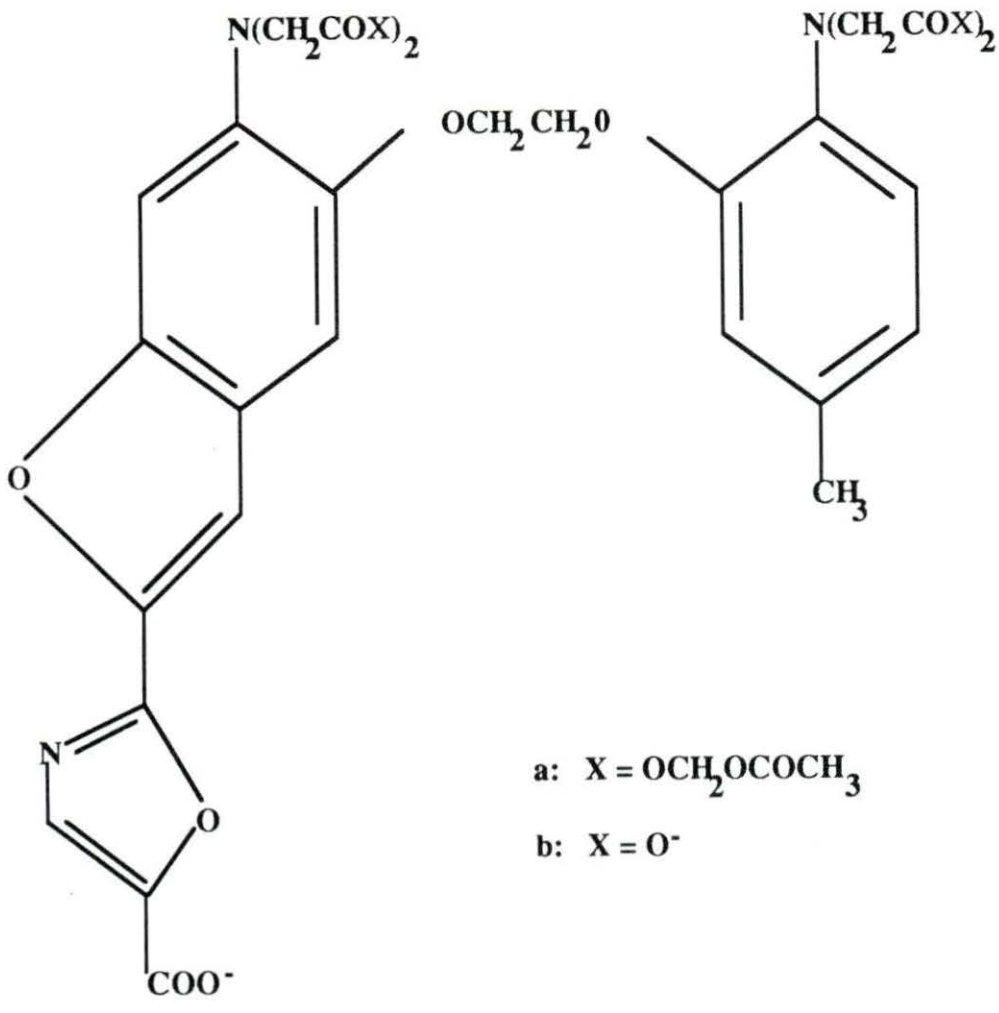

FIGURE 2.2. Structures of Fura-2

a) and its acetoxymethyl tetraester Fura-2/AM.

b) hydrolysis of the ester yields the Fura-2 tetra anion, four molecules each of acetate and formaldehyde, and eight protons.

From Tsien [1981]

In summary, Fura-2 has four main advantages over Quin-2 and other optical indicators. (1) The effective K_d of Fura-2 is approximately two times higher than Quin-2. This lower affinity for calcium enhances the sensitivity of Fura-2 to detect variations in $[Ca^{2+}]$ from 0.1 to 15 μM. (2) Fura-2 fluoresces quite strongly in comparison to Quin-2 because it has a higher quantum efficiency and a much higher extinction coefficient. Therefore, effective fluorescence signals can be detected with approximately 1/30 the concentrations of Quin-2 required to obtain a similar signal. This is important in terms of minimizing calcium buffering, thereby recording fast $[Ca^{2+}]$ transients with little damping, and in terms of minimizing the toxic effects from esterase hydrolysis. (3) Not only does Ca^{2+} change the fluorescence intensity upon binding with Fura-2, but it also changes the excitation wavelengths; only the former situation is true in the case of Quin-2. This property enables calculation of $[Ca^{2+}]$ by the ratio of fluorescence intensities at 340 and 380 nm. This is believed to cancel effects due to variations in instrument efficiency, cell thickness, optical path length, and dye concentration. (4) Fura-2 has better selectivity against Mg^{2+} and heavy metal ions than does Quin-2.

Fura-2 in blood platelets

The studies done on human blood platelets using Fura-2 have confirmed observations made by similar experiments utilizing Quin-2 [Sage and Rink, 1986; Hallam and Rink, 1985]. When Fura-2-loaded platelets were activated with ADP, a rapid increase in $[Ca^{2+}]_i$ was recorded in the absence and presence of extracellular Ca^{2+}. Only 4 μM of Fura-2/AM was required to obtain similar results to those from platelets incubated with 15 μM of Quin-2/AM [Hallam and Rink, 1985; Sage and Rink, 1986].

Early studies used platelets in suspension in a cuvette and $[Ca^{2+}]_i$ was measured using a Perkin Elmer MPF44 spectrophotometer with exciting radiation at 339 nm and emission at 500 nm [Sage and Rink, 1986]. The averaged data from cell suspensions could, however, discount the possibility of a subpopulation of platelets not responsive to ADP. Because the advantages of Fura-2 over previous Ca^{2+} indicator dyes make this dye most appropriate for the study of single cells by fluorescence microscopy, ratio image processing was applied to the study of single platelets [Hallam et al., 1986]. The homogeneity of platelet responses to ADP could therefore be investigated. With 20 μM ADP, a rapid rise in $[Ca^{2+}]_i$ from 100-200 nM to a peak within 1-2 seconds of about 1μM

in > 90% of the cell population was observed [Hallam et al., 1986]. The recording system, described by Williams et al. [1985], used a Silicon Intensified Target (SIT) camera, whose output was digitized to a resolution of 512 x 480 pixels (picture elements) by a video analyzer, with each point in the image assigned a grey value from 0 to 255, depending on intensity. A PDP-11/23 microcomputer digitally analyzed the images. Fluorescence images at 500 nm emission were obtained with 340 and 380 nm exciting radiation. The 340/380 ratio was achieved from a division of the images on a pixel-per-pixel basis after corrections had been made for the background fluorescence in the absence of Fura-2.

The use of Fura-2 as a Ca^{2+} indicator has become widespread over the past five years. It has been used in a variety of other preparations such as smooth muscle cells, parathyroid glands, and Purkinje cells [Williams et al., 1985; Pritchard and Ashley, 1986; Fukuo et al., 1986; Nemeth et al., 1986; Connor et al., 1987; Tank et al., 1988]. However, its limitations must be kept in mind:
(1) The excitation wavelengths of Fura-2 also excite cell autofluorescence which needs to be subtracted from Fura-2 fluorescence before forming the (340/380) ratio.
(2) Fluorescence can be artifactually perturbed by aspects of the intracellular environment such as

viscosity, temperature, and quenching agents [Tsien et al., 1985; Williams et al., 1985; Tsien, 1986].
(3) Measurement of $[Ca^{2+}]_i$ is achieved by comparison of the experimentally determined (340/380) ratio to that from calibration solutions of known Ca^{2+} concentrations. The applicability of this method relies on the assumptions that the exact intracellular dye concentration is known, the dye behaves the same inside the cell as in the calibrating media, the dye molecules are oriented randomly or are sufficiently dilute to record isotropic fluorescence emission in all directions, and fluorescence is linearly proportional to the concentration of the dye. (4) The Fura-2 buffering effect on Ca^{2+} causes some damping of fast $[Ca^{2+}]$ transient changes since more Ca^{2+} is required to reach the usual concentration. This limitation is not very serious since cells normally contain highly efficient calcium buffers. (5) The extinction coefficient of Fura-2 (33×10^3 cm^{-1} M^{-1}), although much higher than that of Quin-2, is lower than that of fluorescein (60×10^3 cm^{-1} M^{-1}) by approximately a factor of 2 [Waggoner, 1986]. Because of this property, Fura-2 fluorescence can only be viewed through high sensitivity cameras whereas that of fluorescein may be viewed with regular video cameras.

CHAPTER THREE: MATERIALS AND METHODS

This chapter describes platelet preparation and loading with Fura-2/AM (acytoxymethyl tetraester), the design and instrumentation of the temperature controlled cell chamber, the digital image processing hardware, and the experimental procedures used to obtain the data.

Platelet Preparation

The preparation of platelets involves the collection of blood samples, the extraction of platelet-rich plasma, and the washing of these platelets in physiological saline.

Blood sample collection

Blood was collected from the cephalic vein of physically restrained, unanesthetized dogs. Plastic syringes containing 3.8% sodium citrate at a ratio of nine volumes of blood to one volume anticoagulant [Matthews, 1987; Rao et al., 1983] were used. The anticoagulant contained trisodium citrate, citric acid, and dextrose at concentrations of 2.5, 1.5 and 2 g/100 mL, respectively. This procedure gave a final whole blood citrate concentration of 22 mM and a measured pH of 6.7 [Hallam and Rink, 1985].

Preparation of platelet-rich plasma

Blood was transferred into polystyrene tubes and centrifuged at 700g for 5 minutes at room temperature [Clemmons and Meyers, 1984]. The speed of the centrifuge in gs was calculated according to the following equation, $g = (11.28 \times 10^{-6}) \times (\text{radius of centrifugation head in cm}) \times (\text{speed in rpm})^2$ [Wolf et al., 1973]. The radius was measured at 7.5 cm, and the speed in rpm was 2870 as measured by a strobe light. The platelet-rich plasma was transferred to a polystyrene tube which was then tightly capped.

Washing of platelets

The platelets were pelleted by centrifugation at 350g, calculated as above with rpm measured at 2030, for 20 minutes at room temperature. The supernatant was discarded using a Pasteur pipette. The pellet was gently resuspended in 1 mL physiological saline of the following composition: NaCl, KCl, $MgSO_4$, HEPES (4-(2-Hydroxyethyl)-1-Piperazine-Ethane-Sulphonic Acid), and dextrose at concentrations in mM of 145, 5, 1, 10, and 10, respectively, and pH 7.4 at 37 °C as was done by Hallam et al. [1984]. The pH of the HEPES buffered solution was adjusted with NaOH to 7.4 at 37 °C. The pH was measured using a Model 10 Corning pH Meter. The pH was adjusted at 37 °C rather than at room temperature

because the pH of the HEPES buffered solution changed as a function of temperature. The - 0.014 (delta) pK/ °C was considered in determining the operating pH [Shipman, 1969]. K is the ionization constant defined as $K = [H^+][A^-]/[HA]$ where A^- represents any anion, and HA is the undissociated acid. The pH changed as a function of pK according to the Henderson-Hasselbalch equation: $pH = pK + \log [A^-]/[HA]$.

Platelets, suspended in HEPES buffered solution, were then left at room temperature in a polystyrene tube prior to loading them with Fura-2/AM.

Loading of Platelets with Fura-2/AM

The process of loading washed platelets with Fura-2/AM involves two steps:

- preparation of Fura-2/AM in DMSO (dimethyl sulfoxide).
- incubation of platelets in Fura-2/AM.

Preparation of Fura-2/AM in DMSO

Fura-2/AM was obtained as yellow oil (1mg) sealed in a vial. The molecular weight of Fura-2/AM is approximately 1000. The 1 mg Fura-2/AM vial was washed in DMSO, the vial was broken, and the Fura-2/AM was dissolved in 1 mL of DMSO. This produced a concentration of 1 mM of Fura-2/AM in DMSO.

The solution was divided into ten aliquots, each containing 0.1 mL. The aliquots were stored in flame-dried ampules. The stock solutions were kept desiccated at -20 °C until use [Tsien et al., 1982].

The concentration of Fura-2/AM solution in DMSO was diluted 250-fold in HEPES buffered solution to reduce the Fura-2/AM concentration to 4 μM [Sage and Rink, 1986] and produce a ratio of DMSO to buffered solution which did not exceed 0.5% volume/volume [Tsien et al., 1982]. Thus, 24.9 mL of the HEPES buffered solution were added to each 0.1 mL aliquot of Fura-2/AM in DMSO.

Incubation of platelets in Fura-2/AM

The washed platelets were centrifuged for 20 minutes at 350g at room temperature. The platelets formed a pellet at the bottom of the tube, and the supernatant was discarded.

The platelets were resuspended in 1 mL Fura-2/AM (4 μM) solution and incubated for 1 hour at 37 °C (using a Thelco 182 water bath). The platelets were then collected by centrifugation at room temperature and resuspended in HEPES buffered solution. Platelets were allowed to equilibrate for a minimum of 15 minutes [Sage and Rink, 1986; Rao et al., 1985; Pollock et al., 1986].

ADP as an Agonist

ADP solution was prepared by reconstituting lyophilized adenosine-5'-diphosphate (ADP Reagent: Sigma Chemical Company) with 1 mL deionized water. This yielded a 200 μM solution which was stored in the refrigerator at 2-6 °C until use. A concentration of 20 μM was achieved by diluting the ADP solution tenfold in HEPES buffered solution. The diluted solution was then warmed to 37 °C prior to adding it to the platelets.

Design and Instrumentation of the Temperature Controlled Cell Chamber

A schematic diagram of the temperature controlled cell chamber is shown in Figure 3.1. This was to be used to maintain the platelets at approximately 37 °C during fluorescence measurements. The temperature control mechanism consisted of an aluminum heating surface and a temperature control circuit. The heat source, thermistor probes, and the cell chamber were mounted on a 3" by 2.2" aluminum heating surface as shown in Figure 3.1. The dimensions of the heating surface were chosen to ensure proper mounting of the chamber on the microscope stage, to fit all components mounted, and to minimize thermal loss.

The aluminum surface was thermally isolated from the microscope stage by two plexiglass strips adhered to the

bottom of that surface. The 0.4" hole acted as a window above which the cell chamber rested; this allowed a wide field of platelets to be monitored through the microscope objective.

The circuit was composed of a 4 Ω, 25 Watt power resistor powered by a DC power supply and a YSI (Yellow Springs Instruments) Thermistep Model 63RC Temperature Controller. The temperature controller acted as a relay switch. To avoid the arcing associated with relay switching, a 10 Ω resistor in series with a 0.1 μF capacitor was connected in series between the "load power" and the "normally closed" terminals as shown in Figure 3.1.

Temperature was sensed by two thermistor probes. The thermistor probe located by the resistor was used as the sensor for the YSI Temperature Controller, while the other was used to monitor the cell chamber temperature.

The resistor and probe placements shown in Figure 3.1, the setting of the coarse and fine controls on the Temperature Controller, and the choice of 8.8 Watt output power were optimized to achieve a 37 °C ± 0.1 °C temperature at the cell chamber site as measured by a YSI Model 47 Scanning Tele-thermometer and the thermistor probe atop the cell chamber cover slip. Thermistor probes and the resistor were coated with a thin film of silicone

heat sink compound to improve thermal contact.

The cell chamber

The cell chamber, a 27 X 46 mm microscope glass slide with a 0.05 mm well cast into the slide, was manufactured by Buehler Ltd. (Catalog number 40-8001 AB "WELL", discontinued). The chamber was covered by a 22 X 40 mm glass cover slip. The microscope slide as well as the cover slip were coated with Formvar to prevent platelet activation by the glass. Formvar coating was done as outlined by Moran et al. [1987]. The cell chamber was mounted loosely on the aluminum plate with the hole forming the window centered beneath it.

Digital Image Processing Hardware

The digital image processing hardware utilized to record and analyze Fura-2 fluorescence consisted of the following:

- a Zeiss Axiophot Fluorescence microscope
- a Silicon Intensified Target (SIT) camera.
- a Zeiss image analyzer

This system, which is an adaptation of the one utilized by Williams et al. [1985], is schematically shown in Figure 3.2.

The fluorescence microscope

The Zeiss Axiophot Fluorescence microscope with its epi-fluorescence condenser unit is diagramed in Figure 3.3. A Zeiss Plan-Neofluar 100X oil immersion objective lens with a 1.30 numerical aperture was used in fluorescence imaging. The SIT camera was mounted above the barrier filter as shown in Figure 3.3.

The epi-fluorescence condenser unit Basically, epi-fluorescence is a method by which light passes through the microscope objective to and from the specimen [Gray, 1973]. The condenser unit is shown in Figure 3.4. It has (1) a HBO 50-Watt high pressure mercury lamp as the source of the ultraviolet (uv) exciting radiation and a heat absorption filter to protect the excitation filters and the specimen from the high temperature generated by the mercury lamp (2) the excitation filters and (3) a reflector housing.

The excitation filters are 18 mm diameter interference filters having 340 and 380 nm transmission peaks, each with a half-bandwidth of 13 nm (Omega Optical: 340 DF 10; 380 DF 10). The transmission curves for these filters are shown in Figure 3.5 and Figure 3.6.

The reflector housing consists of (1) a 45° angled interference filter acting as a chromatic beam splitter and (2) a 420 nm long pass barrier filter whose

transmission curve is shown in Figure 3.7. According to the manufacturer (Zeiss), the beam splitter, coded FT 395, has a cutoff of 395 nm. The transmission curve of the beam splitter is shown in Figure 3.8. Therefore, exciting radiation below 395 nm is reflected onto the Fura-2/AM-loaded platelets, while wavelengths above 395 nm are allowed to pass through the beam splitter to strike the barrier filter as shown in Figure 3.9.

The SIT camera

A silicon intensified target (SIT) camera (SIT: Dage MTI Model 66X) was used to acquire fluorescent images from the microscope. This camera can function with low input light levels and can also be used for continuous on-line recording [Reynolds and Taylor, 1980].

The two properties mentioned are important in fluorescence microscopy. Fluorescence from Fura-2-loaded platelets is low, especially at 340 nm exciting radiation and, therefore, is difficult to detect with conventional T.V. cameras. The on-line continuous recording property enables fluorescence recording with limited time exposure to exciting radiation. This limits dye-bleaching and photodynamic damage that would otherwise occur from prolonged exposure [Cohen and Lesher, 1986].

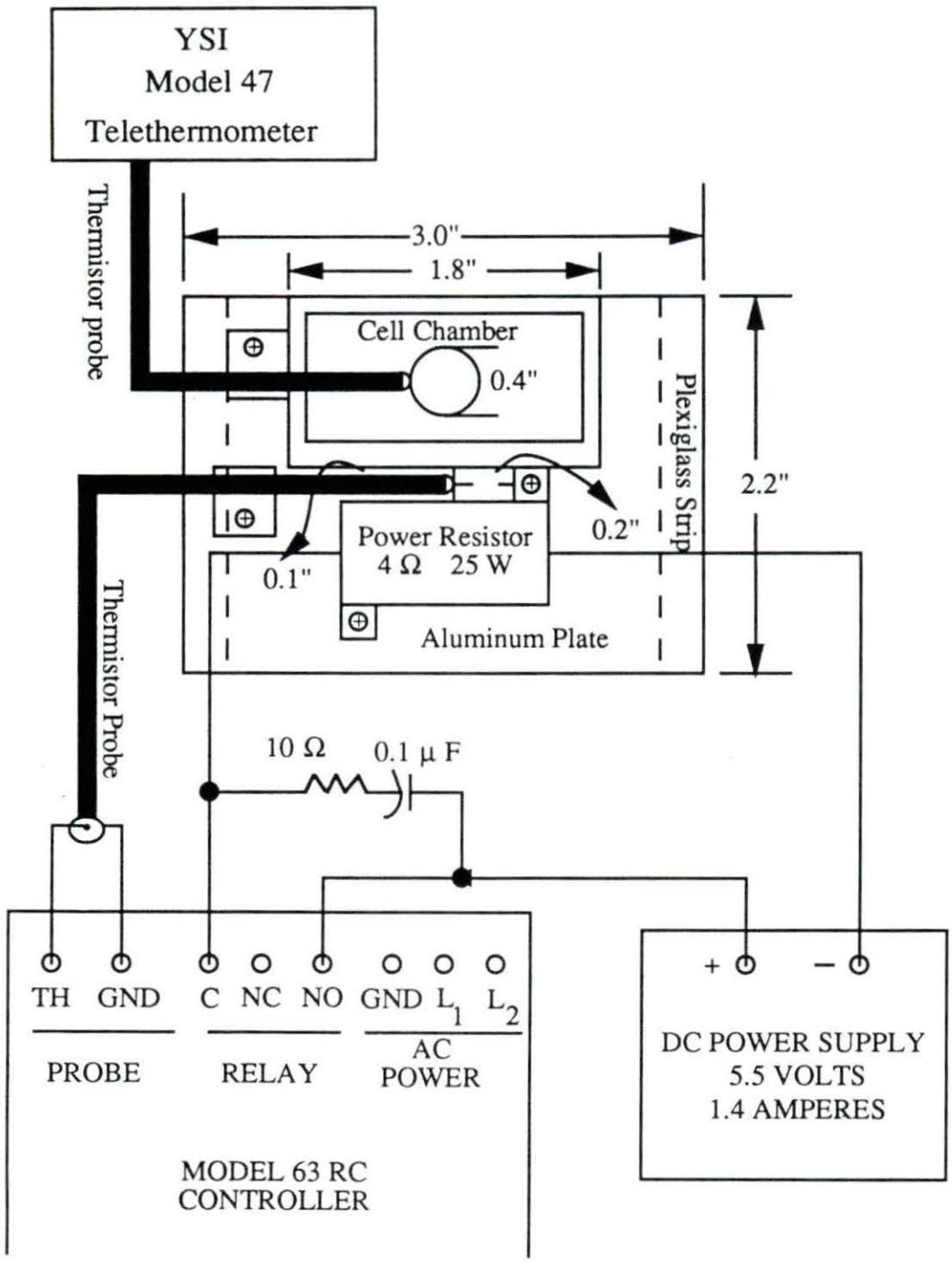

FIGURE 3.1. Temperature controlled cell chamber

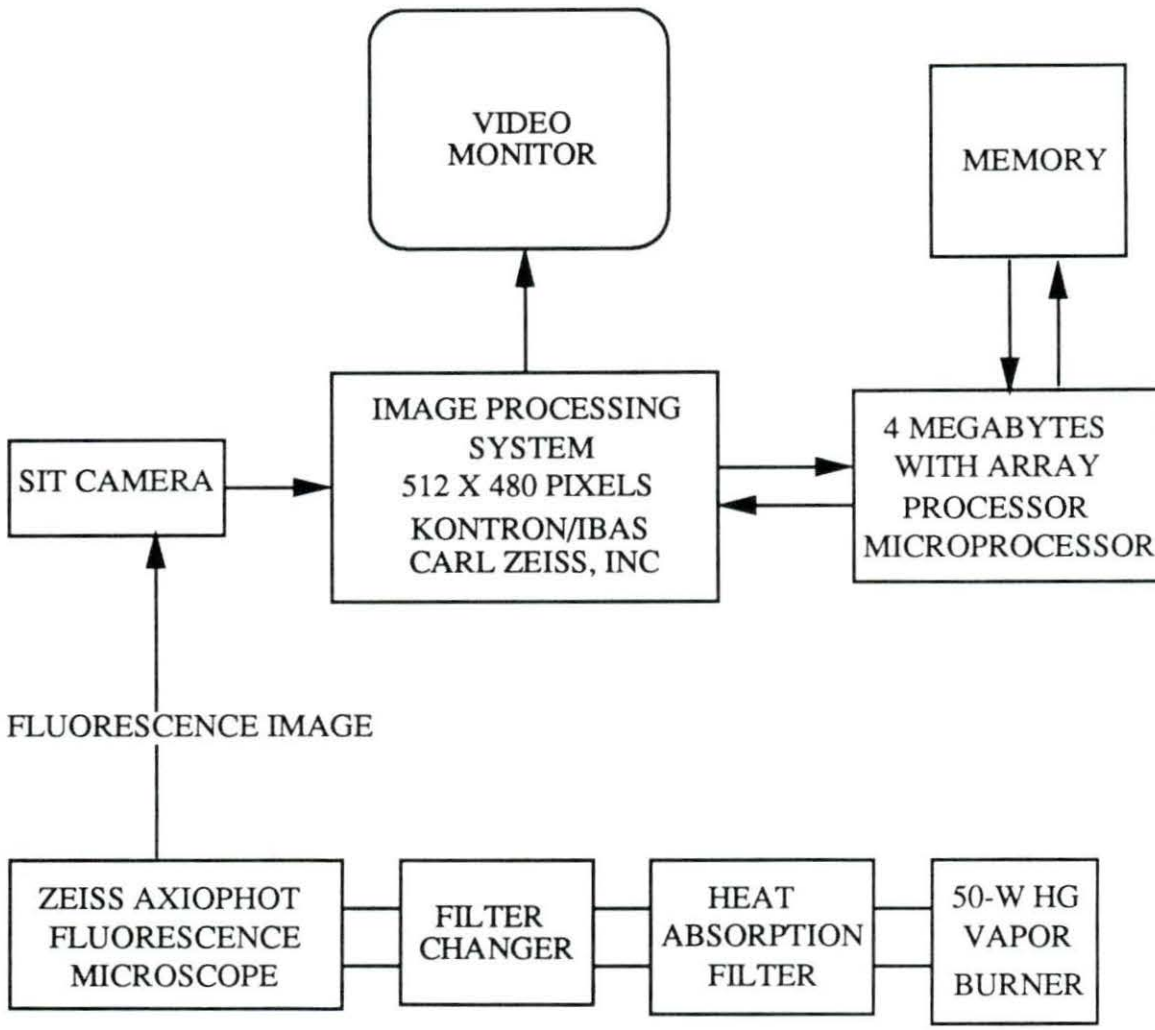

FIGURE 3.2. Block diagram of the digital image processing hardware

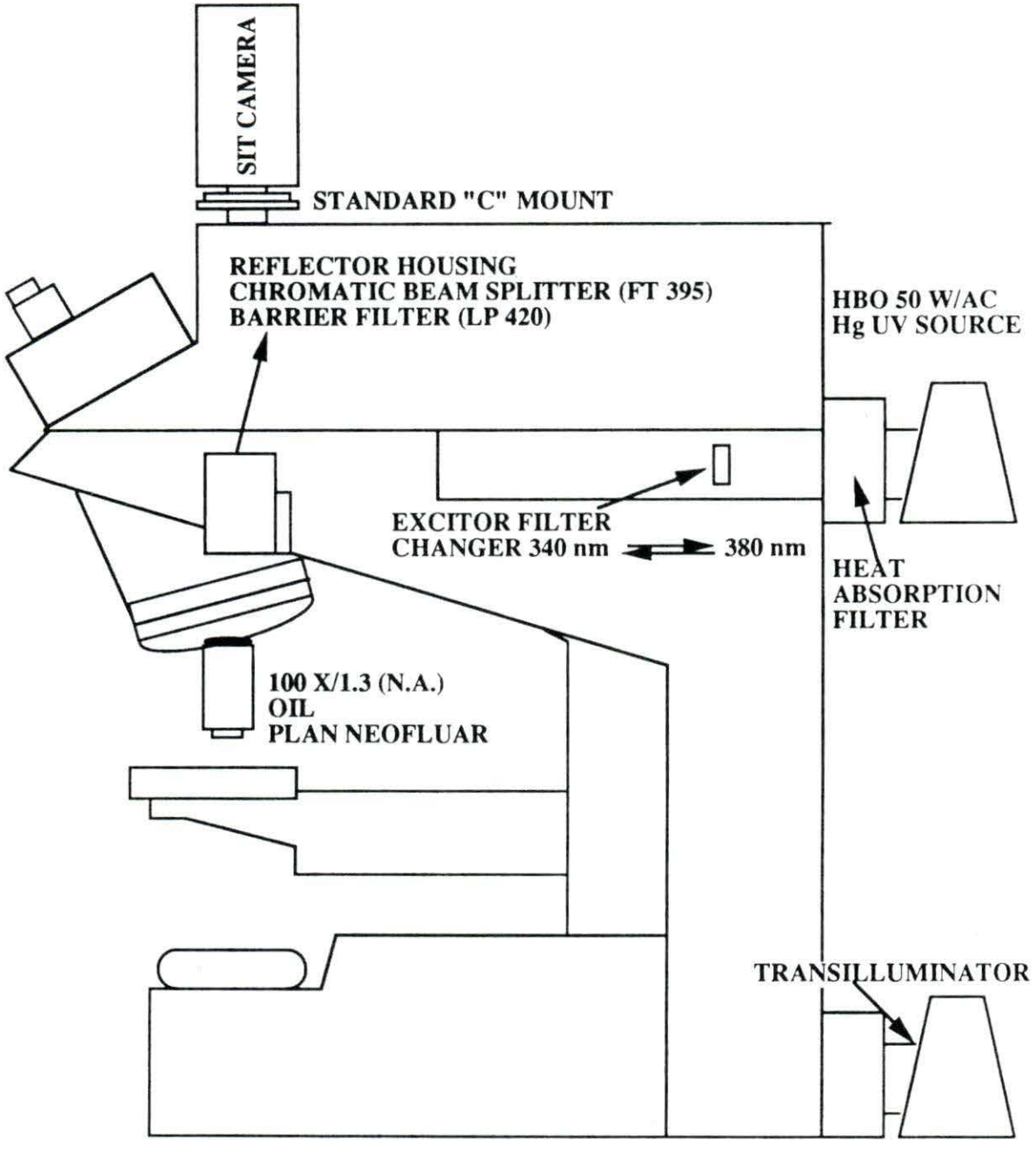

FIGURE 3.3. Schematic diagram of the Zeiss axiophot fluorescence microscope with the epi-fluorescence condenser unit and SIT camera

From Zeiss Systems Chart Axiophot Photomicroscope

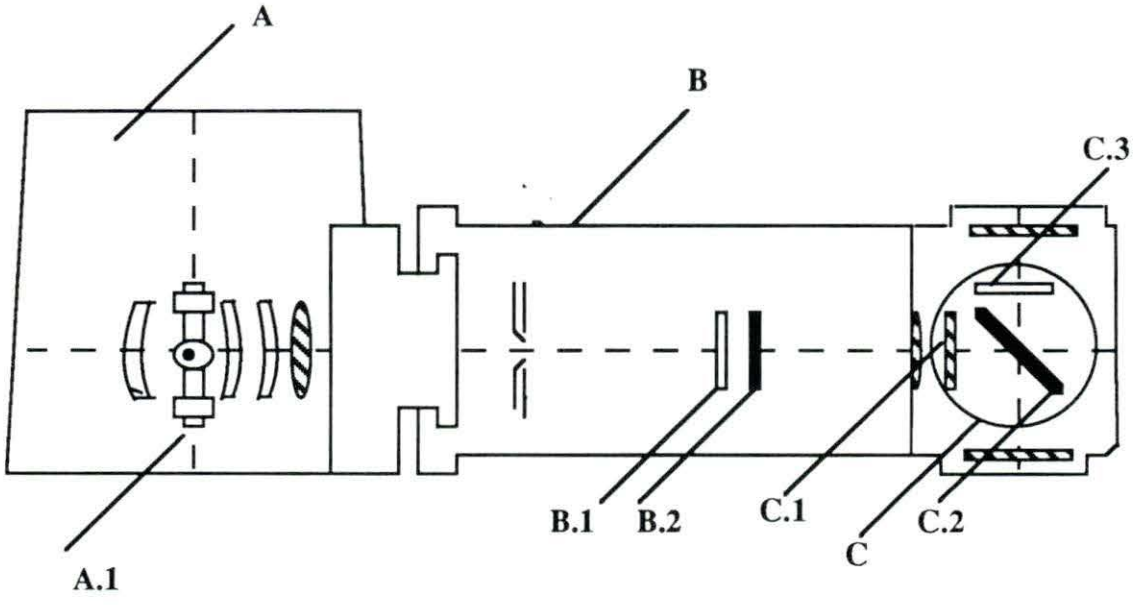

FIGURE 3.4. Schematic diagram of the epi-fluorescence condenser unit

A. HBO 50-Watt high pressure mercury lamp

A.1 Light source

B. Illuminating tube

B.1 Heat absorption filter

B.2 Three-position slider filter changer

C. Reflector housing unit

C.1 Excitor filter

C.2 Reflector, a 45°chromatic beam splitter

C.3 Barrier filter

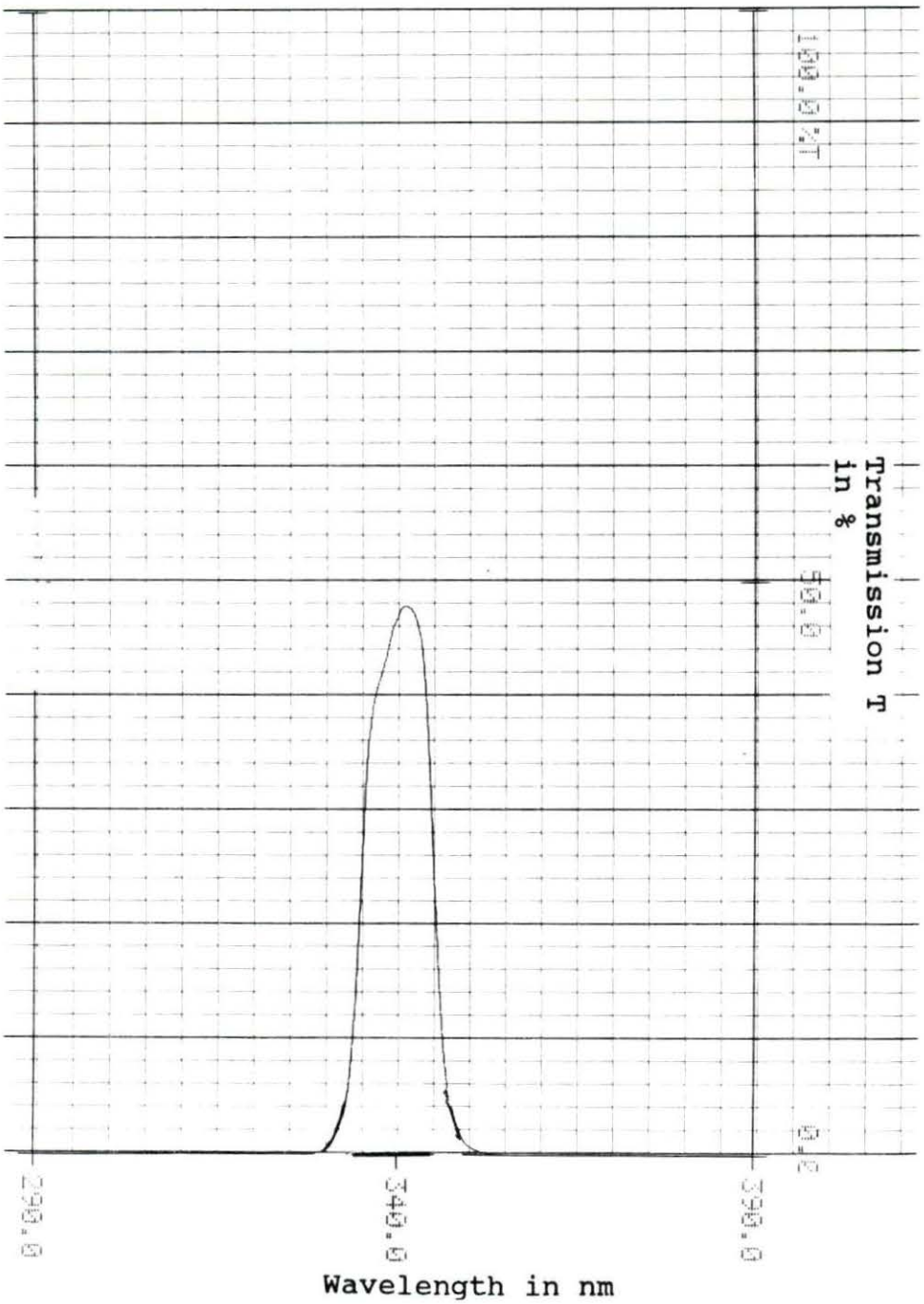

FIGURE 3.5. Fura-2 340 nm excitor filter transmission curve

From Omega Optical, Brattleboro

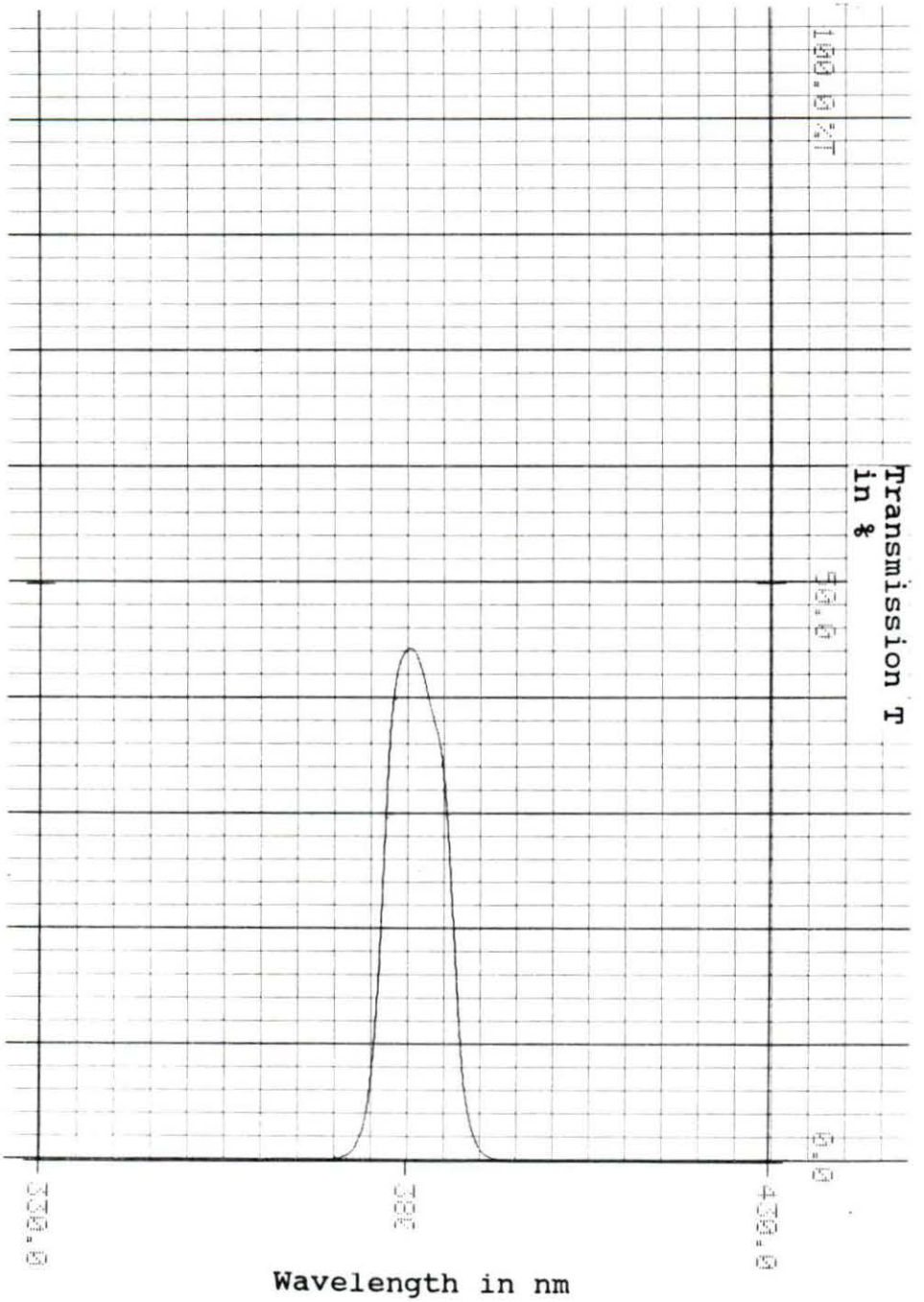

FIGURE 3.6. Fura-2 380 nm excitor transmission filter curve

From Omega Optical, Brattleboro

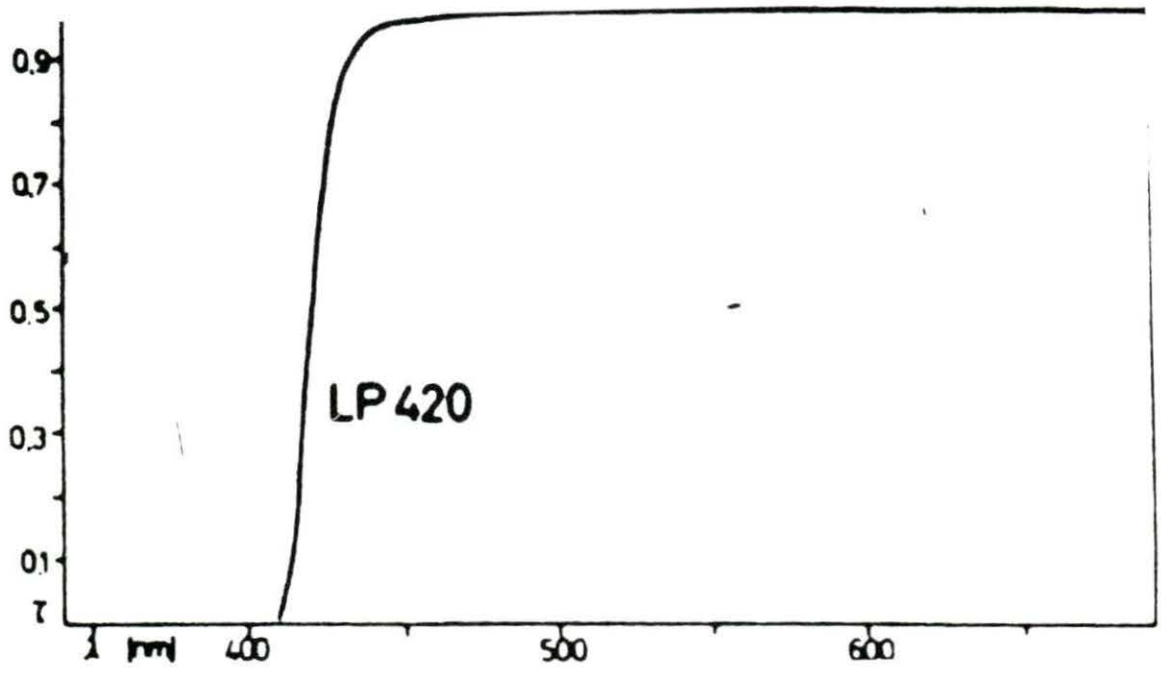

FIGURE 3.7. Transmission curve of the 420nm long pass (LP 420) barrier filter

From Zeiss filter specifications

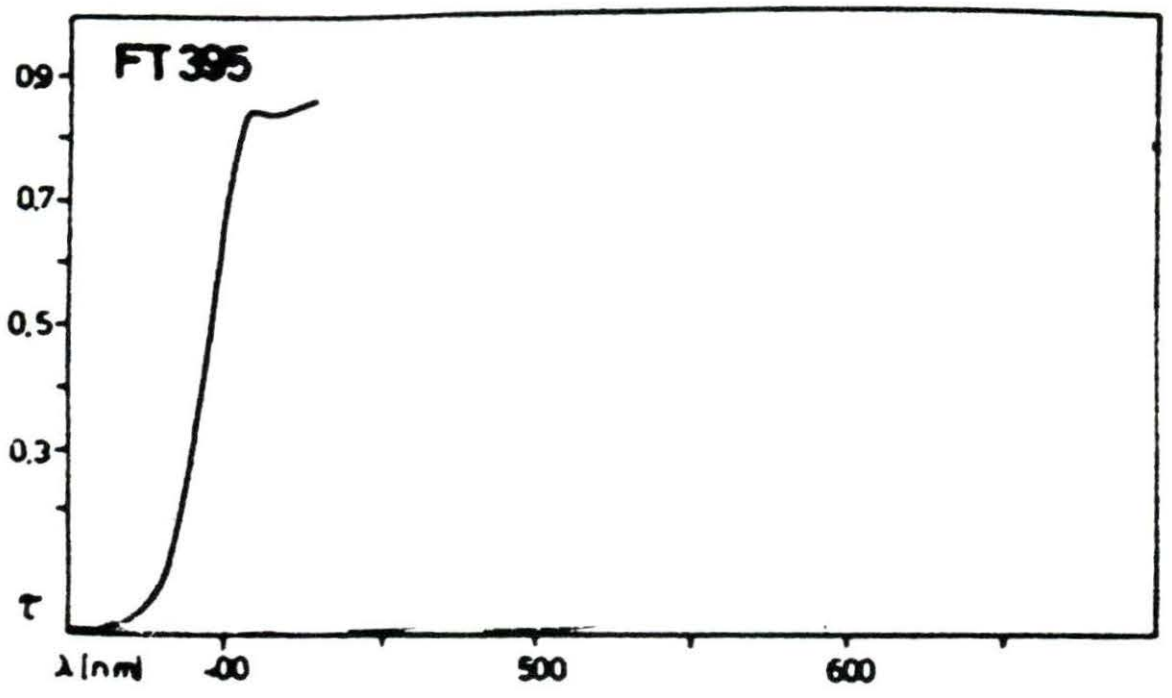

FIGURE 3.8. Transmission curve of the 395nm dichroic beam splitter (FT 395)

Adapted from Zeiss filter specifications

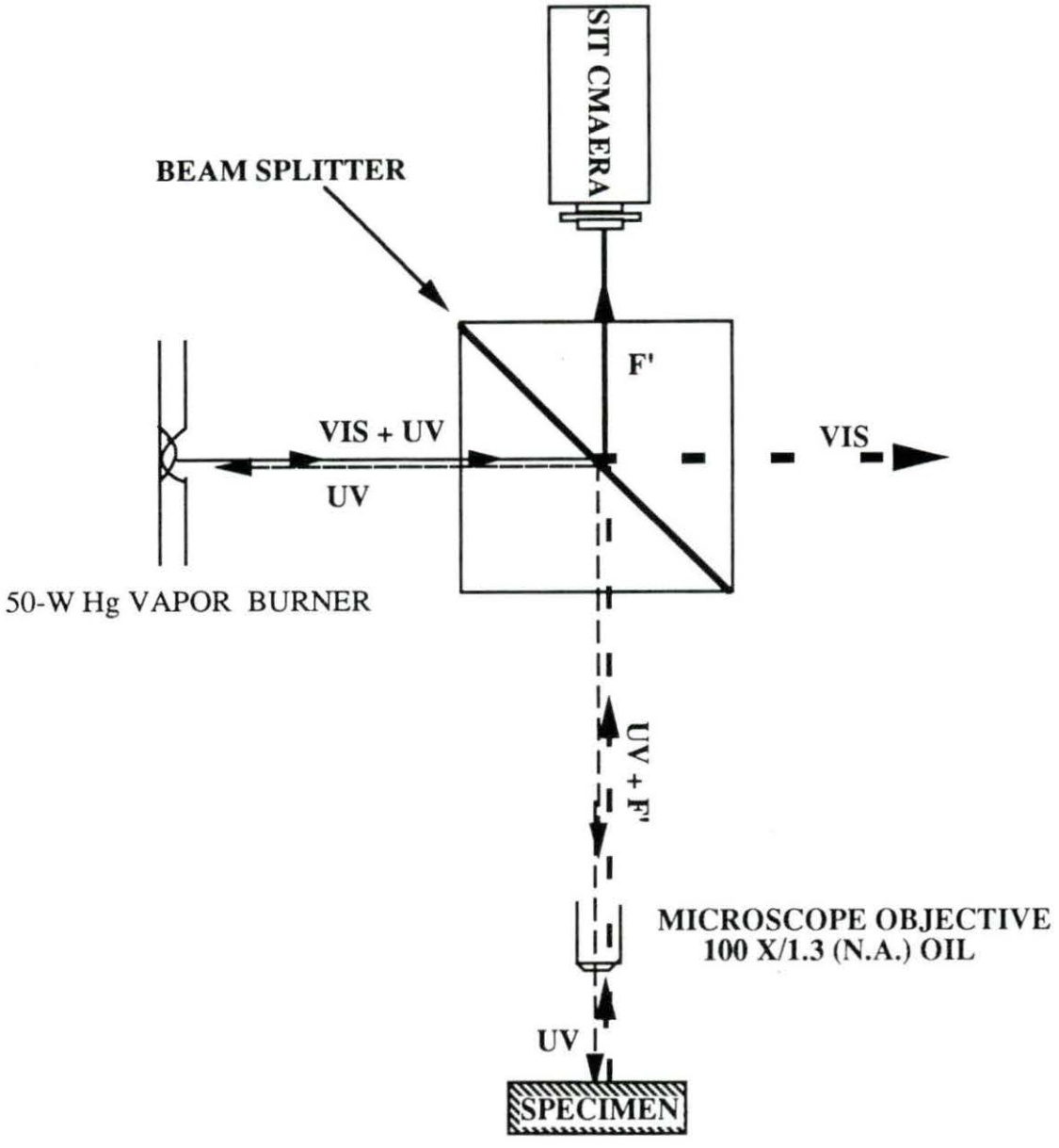

FIGURE 3.9. Partition of exciting and fluorescence light by an interference layer incident-light fluorescence

uv = ultra-violet radiation

VIS = visible primary light

F' = fluorescence

From Gray [1973]

The image processing system

The output of the SIT camera was digitized to a resolution of 512 x 480 pixels (picture elements) by a Zeiss Image Processing system. This system is comprised of an IBM-compatible microcomputer equipped with an array processor, a 4 megabyte hard disk, and a Zeiss video monitor. This system was used to perform the following functions [Fay et al., 1986]:

- to quantify each digitized point in the image by assigning it a grey value from 0 to 255, depending on image intensity.
- to store the digitized images at the 340 and 380 nm exciting radiations.
- to perform ratio operations of images ($R_{340/380}$) and then to store the resulting image.
- to enhance the images recorded.

Methods of Collecting Data

Fura-2-loaded platelets were transferred to the temperature controlled cell chamber using a 100 μL plastic micropipette. However, it was observed that images seen through the oculars were drifting in and out of focus. This was attributed to flexure in the temperature controlled chamber mechanism because of thermal stress. This focus drift was eliminated when the aluminum heating

plate was removed. Subsequently, experiments were conducted at room temperature. Platelets were left in the covered chamber for approximately five minutes to allow them to settle and adhere to the bottom of the chamber.

Transillumination by visible light was employed to locate and focus individual platelets. The sample was exposed to transillumination for a very short period, approximately 30 seconds, in order to minimize dye-bleaching. The sample was then exposed to the 380 nm exciting radiation and viewed through the microscope oculars. The oculars were then occluded and the SIT camera was exposed to the platelets' fluorescence. The SIT camera was operated in manual mode with two different settings: one for the fluorescence due to 380 nm exciting radiation, and the other for fluorescence due to 340 nm exciting radiation. The image obtained from the camera was digitized by the video analyzer and displayed on the video monitor. The focus was readjusted until a sharp image was observed on the monitor. This adjustment was necessary because the microscope and the camera were not parfocal.

The 380 nm fluorescent image was recorded on the image analysis system and the recording procedure was repeated to obtain the fluorescent image of the sample at the 340 nm exciting radiation. The time delay between the

two images was approximately 30 seconds. This delay was due to the time required to manipulate the image processing system and to manually exchange filters for each frame.

ADP solution at 20 μM was diffused through the chamber and images were recorded at 380 and 340 nm exciting radiations. These fluorescent images were of the same platelet field previously examined.

The data acquisition process described above was repeated for two other platelet samples. Hard copies were then acquired from a laser printer.

CHAPTER FOUR: RESULTS AND DISCUSSION

In this chapter, the results of the previously described experiments are reported and discussed. Observations are also made concerning the optical system used and Fura-2/AM fluorescence and loading behavior in platelets.

Experimental Data

The printed images collected by the methods described in Chapter Three were distorted in intensities because of the printer limitations and thus did not represent the images seen on the video monitor. These raw data are available in the Appendix as Figures A.1 through A.6.

In order to produce visually interpretable images and their respective ratios, image enhancement was required. Image enhancement was accomplished by increasing contrast between the dark background and the bright images which represented fluorescing platelets. This process expanded the images' grey values by a linear one-to-one mapping to enhance their brightness. For example, if the grey value of the brightest pixel in a given field was 100, then multiplying it by 255/100 would assign this image a grey value of 255. Subsequently, all other pixel intensities would be expanded. This process is called "histogram contrast increase" or "image enhancement".

Mathematically, "image enhancement" can be expressed by:

$$INT^{*}(x,y) = L \times INT(x,y)$$

where x and y are the pixel coordinates;

$INT^{*}(x,y)$ is the enhanced grey value of the pixel;

INT(x,y) is the unenhanced grey value of the pixel;

L = 255/MAX(INT(x,y)) is the transformation multiplier;

MAX(INT(x,y)) is the maximum grey value in the given field.

The enhanced images are shown in Figure 4.1 through Figure 4.6. Since each image frame had a different histogram of grey values, the multipliers had to be different from one enhanced image to another. It is emphasized that grey values used as quantitative data in subsequent discussion were obtained from the unenhanced images.

Fura-2-loaded platelets

The images shown in Figures 4.1a and 4.1b are the enhanced fluorescence images of Sample ONE platelets which were excited at 380 nm and 340 nm, respectively. Figure 4.2 is the ratio ($R_{340/380}$) of these images. The letters used on the Figures denote the images of fluorescent platelets. Identical letters denote identical platelets whether they are images from 380 nm excitation, from 340 nm excitation, or from the ratio ($R_{340/380}$) image. The figure arrangements described above for Sample ONE

platelets are also followed in the descriptions of Figure 4.3 through Figure 4.4 for Sample TWO, and likewise Figure 4.5 and Figure 4.6 for Sample THREE platelets. The number associated with each letter indicates the platelet sample.

■ The image at 380 nm exciting radiation was observed to be brighter than that at 340 nm. This is illustrated by comparing image "A1" in Figure 4.1a to that in Figure 4.1b. Furthermore, this result is consistent in the other two platelet samples. This is also confirmed by observing that the ratio image "A1" in Figure 4.2 is black, a result of dividing the darker 340 nm image by the brighter 380 nm image. Moreover, the actual grey value of the original image "A1" at 380 nm excitation is 170 in comparison to the grey value of 100 at 340 nm. This result should indicate that the concentration of the calcium-free dye is greater than that of the calcium-bound dye (see Chapter Two). This would suggest that the $[Ca^{2+}]_i$ was at the basal level and that the platelets were not activated.

Although these observations suggest that the concentration of the calcium-free dye was higher than the concentration of the calcium-bound dye, other factors are involved that could account for these observations.

1) Background fluorescence was more intense at 380 nm exciting radiation than at 340 nm exciting radiation.

Nevertheless, when platelets were unsuccessfully loaded with Fura-2/AM, background fluorescence was extremely small even at 380 nm excitation. This may indicate that background fluorescence is not a significant factor. 2) It can be argued that the comparisons made between the fluorescence intensities due to 340 nm and 380 nm exciting radiation are relative since R_{min} and R_{max} were not determined. (R_{min} and R_{max} are obtained as described in Chapter Two). Thus, large differences in intensities may actually not be reflective of the calcium levels in the cells. 3) There was an appreciable difference in the excitation intensities between the 380 nm and 340 nm exciting radiation that could account for the difference in fluorescence intensity.

Image "B1" is less intensely fluorescent than image "A1" in Figure 4.1a. This might have been due to platelet "A1" being loaded with a higher concentration of Fura-2 than platelet "B1", or to the $[Ca^{2+}]_i$ in platelet "A1" being lower than that in platelet "B1". The ratio ($R_{340/380}$) images "A1" and "B1" in Figure 4.2 do not provide much contrast in brightness, so it cannot be objectively determined which image was darker. However, observing image "B1" in Figure 4.1a is still distinguishable while image "B1" in Figure 4.1b is not, and observing the ratio image in Figure 4.6, where the

differences in the degree of brightness can be seen, it is more plausible to conclude that the Fura-2 concentration in platelets was not uniform. This is consistent with the report by Tsien [1986] regarding the nonuniformity of dye loading in cells.

Fura-2-loaded platelets in a solution containing ADP

ADP, at a concentration of 20 μM, was diffused into the three platelet samples described earlier. Images at 380 nm and 340 nm exciting radiation, as well as their respective ratio ($R_{340/380}$), were recorded. The images examined showed no change from the corresponding images before adding ADP. It was also observed that the individual platelets in each sample remained adherent to the formvar-coated glass of the cell chamber. The fact that no change occurred after adding the agonist ADP is inconsistent with the reports by Hallam and Rink [1985], Hallam et al. [1986], and Sage and Rink [1986] which detected a rise in $[Ca^{2+}]_i$ after the agonist ADP was added. There are several possibilities that could have either singly or collectively accounted for such a discrepancy.

* Platelets were not responsive to ADP at room temperature.

* ADP at 20 μM concentration was not appropriate for platelet activation.

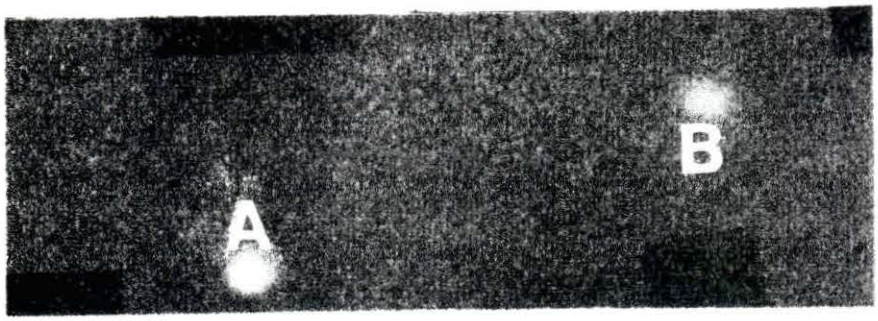

(a)

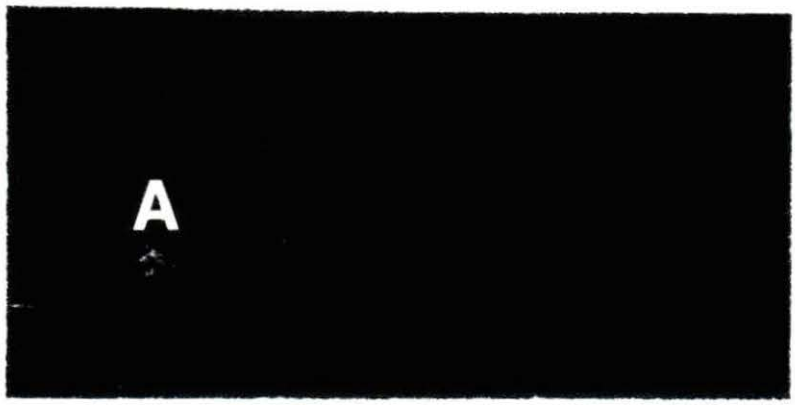

(b)

FIGURE 4.1. Digitally enhanced fluorescence image of Sample ONE platelets due to excitation at:

a) 380 nm exciting radiation

b) 340 nm exciting radiation

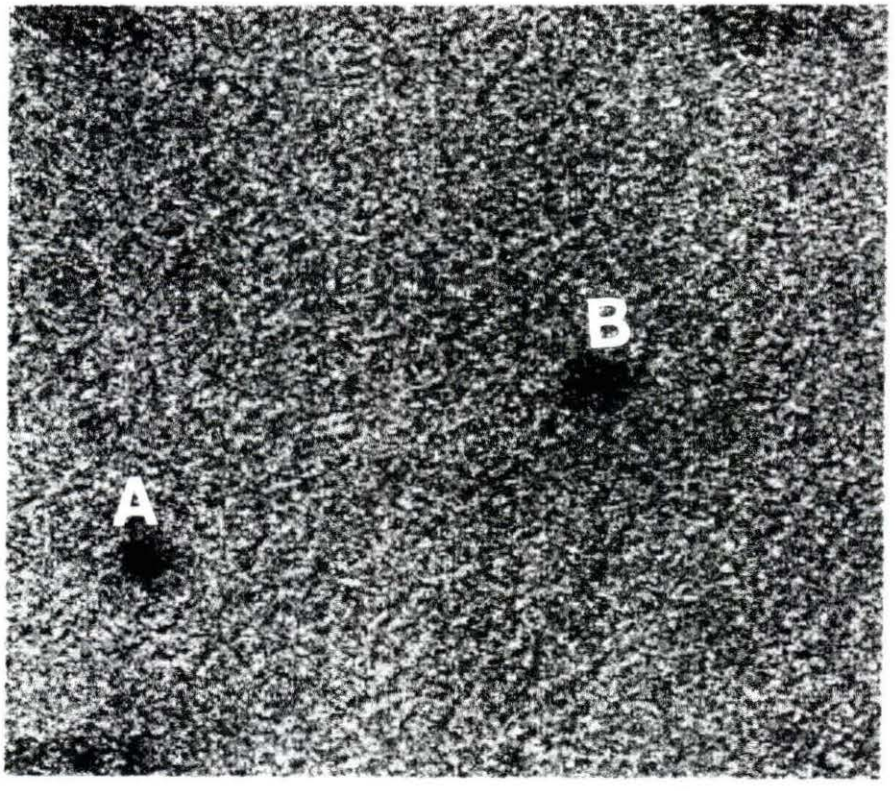

FIGURE 4.2. Digitally enhanced ratio image ($R_{340/380}$) of Sample ONE platelets

The fluorescence image due to 340 nm excitation was divided by that due to 380 nm excitation on a pixel-per-pixel basis

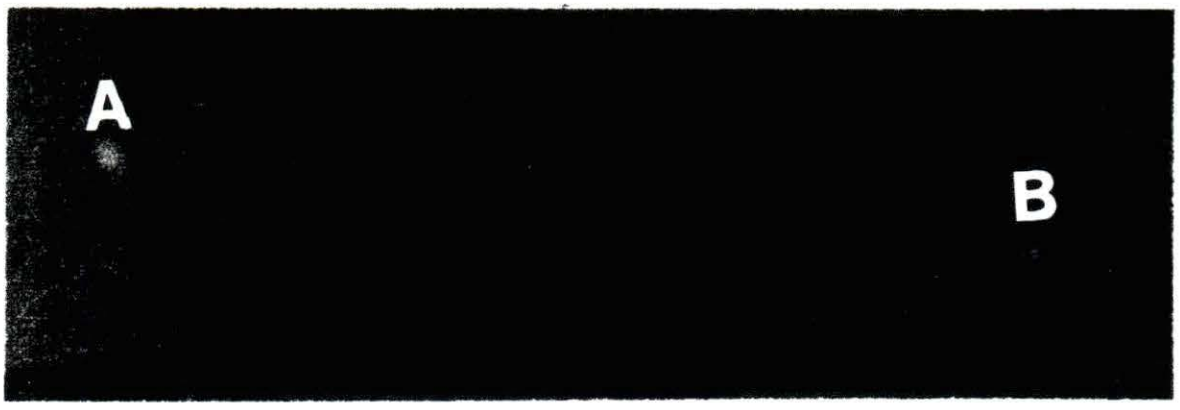

(a)

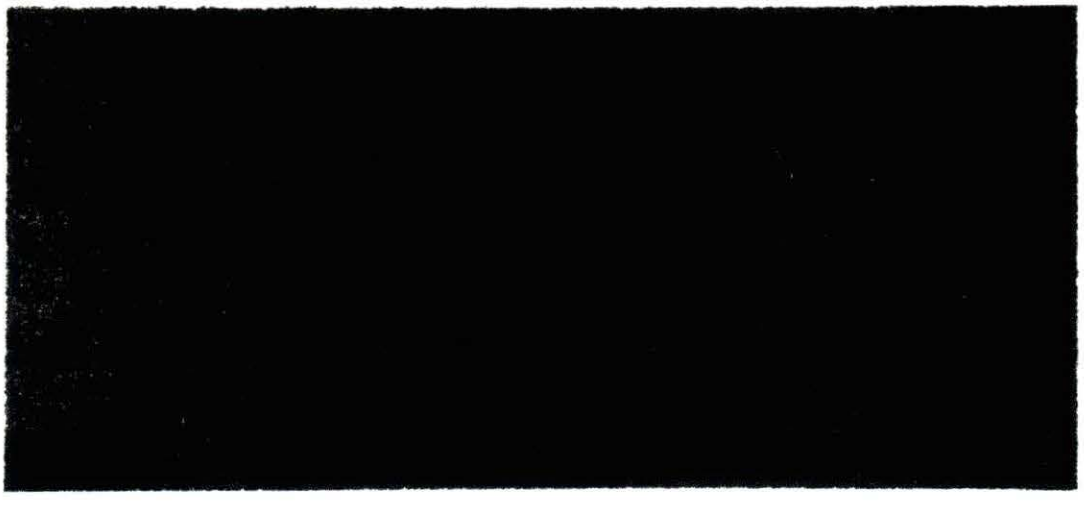

(b)

FIGURE 4.3. Digitally enhanced fluorescence image of Sample TWO platelets due to excitation at:

a) 380 nm exciting radiation

b) 340 nm exciting radiation

FIGURE 4.4. Digitally enhanced ratio image ($R_{340/380}$) of Sample TWO platelets

The fluorescence image due to 340 nm excitation radiation was divided by that due to 380 nm excitation on a pixel-per-pixel basis

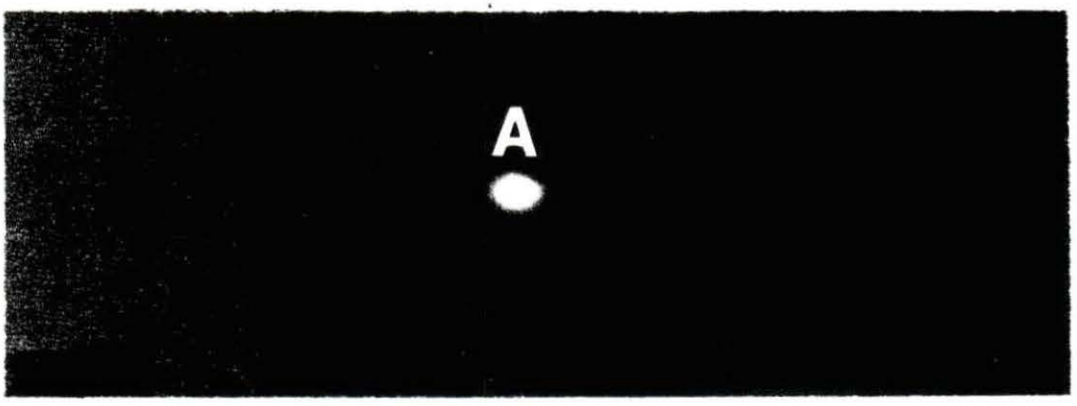

(a)

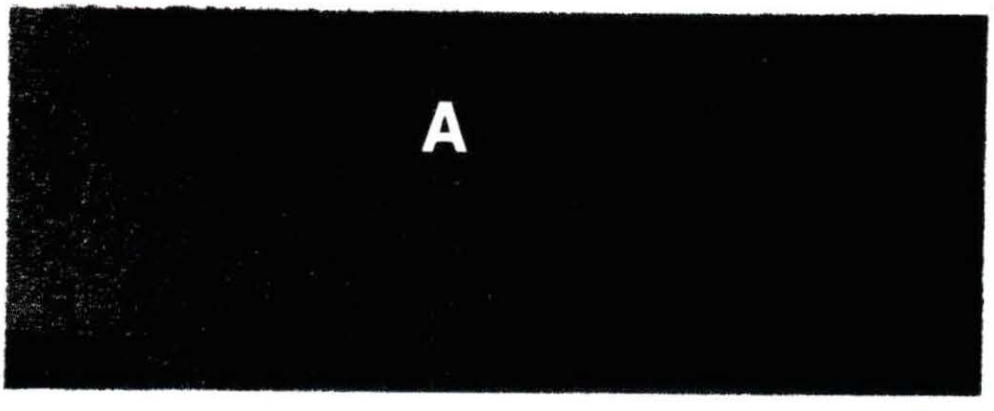

(b)

FIGURE 4.5. Digitally enhanced fluorescence image of Sample THREE platelets due to excitation at:

a) 380 nm exciting radiation

b) 340 nm exciting radiation

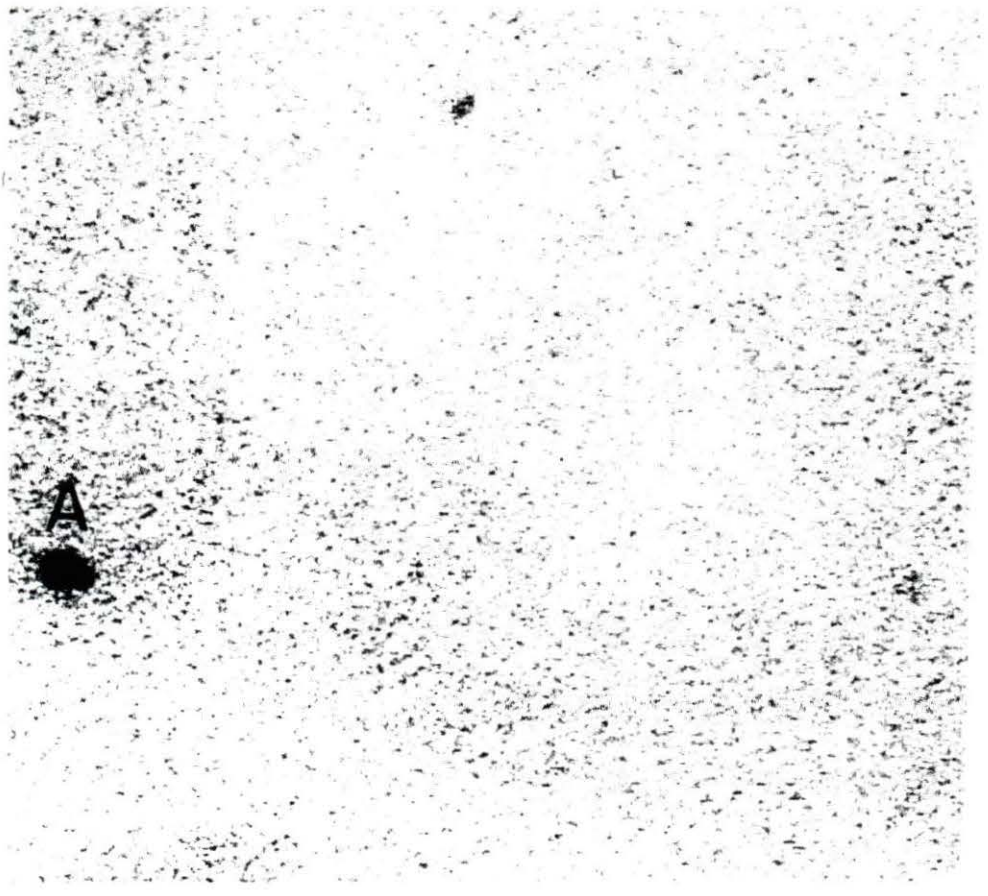

FIGURE 4.6. Digitally enhanced ratio image ($R_{340/380}$) of Sample THREE platelets

The fluorescence image due to 340 nm excitation was divided by that due to 380 nm excitation on a pixel-per-pixel basis

- Platelets were desensitized to ADP because of the agitation caused by centrifugation.

- The difference in intensity of the two exciting radiation wavelengths and the resulting difference in fluorescence intensity may obscure small changes in fluorescence intensity due to changes in calcium concentration.

- Extracellular calcium ions were virtually nonexistent. This may suggest that the major component of the ADP-stimulated rise in $[Ca^{2+}]_i$ is caused by the influx of extracellular calcium ions through the plasma membrane.

The Optical System

The following are observations made, based on several experiments, regarding the 50-W Hg uv source and the filters in the path of the excitation beam, the dichroic mirror characteristics, and some of the properties of the SIT camera used.

The uv excitation source

The spectral output of a typical Hg vapor burner is shown in Figure 4.7 [Gray, 1973]. The output intensity of the Hg lamp is less at 340 nm than at 380 nm. Moreover, the Hg lamp used is rated at 50 Watts. This power output is further reduced by absorption occurring in the path of the uv source. The beam focusing lens, heat absorption

filter, 340 nm filter, dichroic mirror, microscope objective, glass coverslip and specimen together absorb most of the beam intensity. Since the quantum efficiency of Fura-2 is less than 0.5, the resultant fluorescence intensity is very small. This low fluorescence intensity is probably responsible for the low signal-to-noise ratio at 340 nm; therefore, it is concluded that the 50-W Hg lamp is inadequate as a source for uv excitation at 340 nm.

The dichroic mirror

Although, according to the manufacturer, a 460 nm dichroic mirror (Zeiss: FT 460) should reflect all wavelengths below 460 nm and pass, at 90% transmission, all those above 460 nm, preliminary experiments showed otherwise. (See Figure 4.8.) A well-mixed Fura-2/AM solution was placed directly before the dichroic mirror in the path of the excitation beam at 340 nm. The dye fluoresced, emitting a characteristically green light as seen by the naked eye. Fluorescence also occurred at that location at 380 nm excitation. However, when each solution was placed directly underneath the dichroic mirror in the path of the reflected light, no fluorescence was observed at 340 nm excitation, while fluorescence occurred at 380 nm. When the same series of experiments were conducted with a 395 nm dichroic mirror, fluorescence

occurred at both locations and at both excitation wavelengths. These results suggest that the 460 nm dichroic mirror being used absorbed either all or most of the intensity at 340 nm rather than reflecting it. It is concluded that the upper limit of reflection for dichroic mirrors should be chosen slightly above the higher excitation wavelength to be used and that all critical optical components should be tested for their spectral characteristics.

The SIT camera

The camera gain was observed to be sensitive to spatial variations within the specimen. When operated in the automatic gain mode, the SIT camera was saturated by the images of bright fluorescence due to 380 nm excitation. This resulted because the image field was mostly dark except for the relatively small bright images produced by the fluorescing platelets. This problem was overcome by operating the camera in the manual mode. Furthermore, low signal-to-noise ratio images were observed on the video monitor when the camera was operated manually at 340 nm excitation. This was due to the low fluorescence intensity level at this excitation wavelength.

Fura-2/AM Fluorescence and Loading

The following is a qualitative description of the Fura-2/AM "aging" and hydrolysis effects on fluorescence and loading of the dye in platelets.

Fura-2/AM was dissolved in DMSO and stored desiccated and frozen at -20 °C. Over a period of three months, each aliquot was diluted with HEPES buffered solution and warmed to 37 °C immediately before use. After use, the remaining solution was discarded. Fura-2-loaded platelets fluoresced at 380 nm and to a lesser degree at 340 nm excitation wavelengths. Therefore, frozen Fura-2/AM in DMSO solution appeared to be stable over a three month period.

The last Fura-2/AM aliquot was used four times over a period of four weeks. A substantial decrease in fluorescence was noticed over this time period. This was possibly due to "aging" and hydrolysis because of repeated thawing and freezing. This might have also decreased the concentration in platelets.

Fura-2/AM diluted in HEPES buffered solution either loaded poorly or not at all in platelets centrifuged from hemolyzed blood. It was possible that esterases released from the damaged red blood cells actually hydrolyzed most or all of Fura-2/AM into the cell-impermeable Fura-2 acid before it could diffuse into platelets.

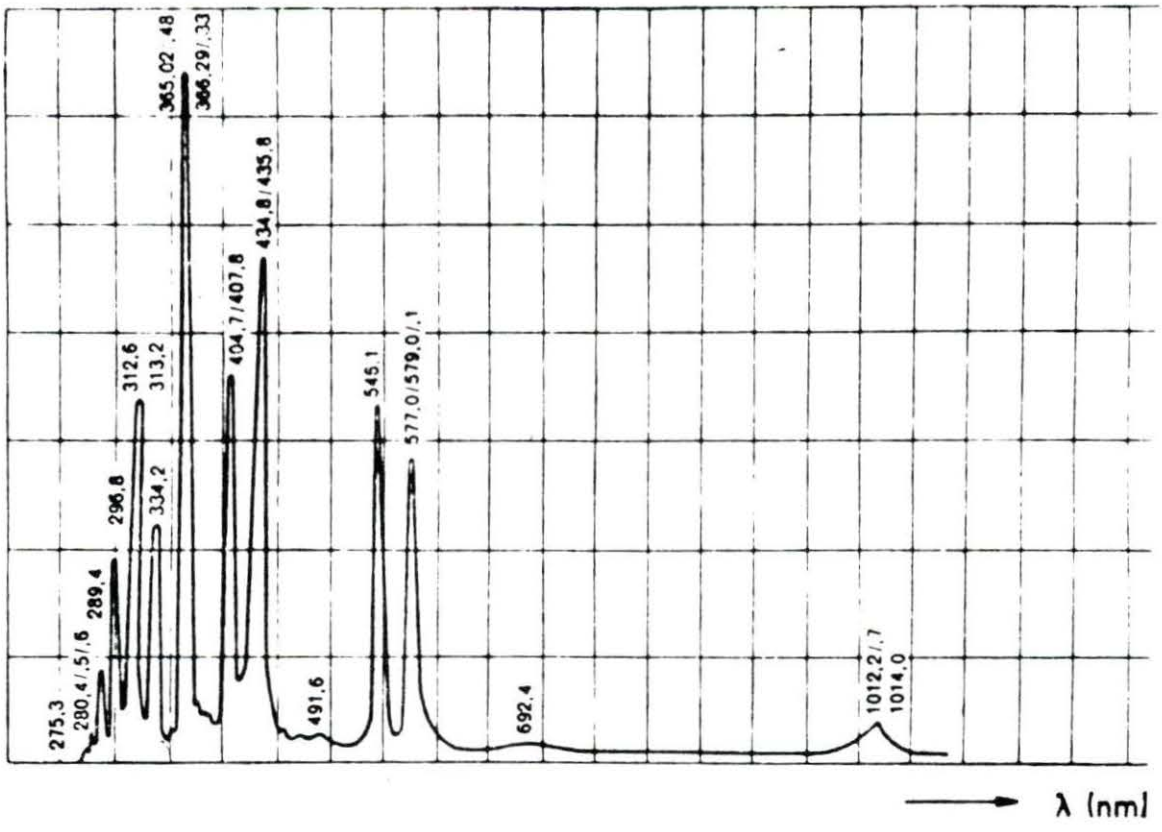

FIGURE 4.7. The spectral output of a typical mercury vapor burner

From Gray [1973]

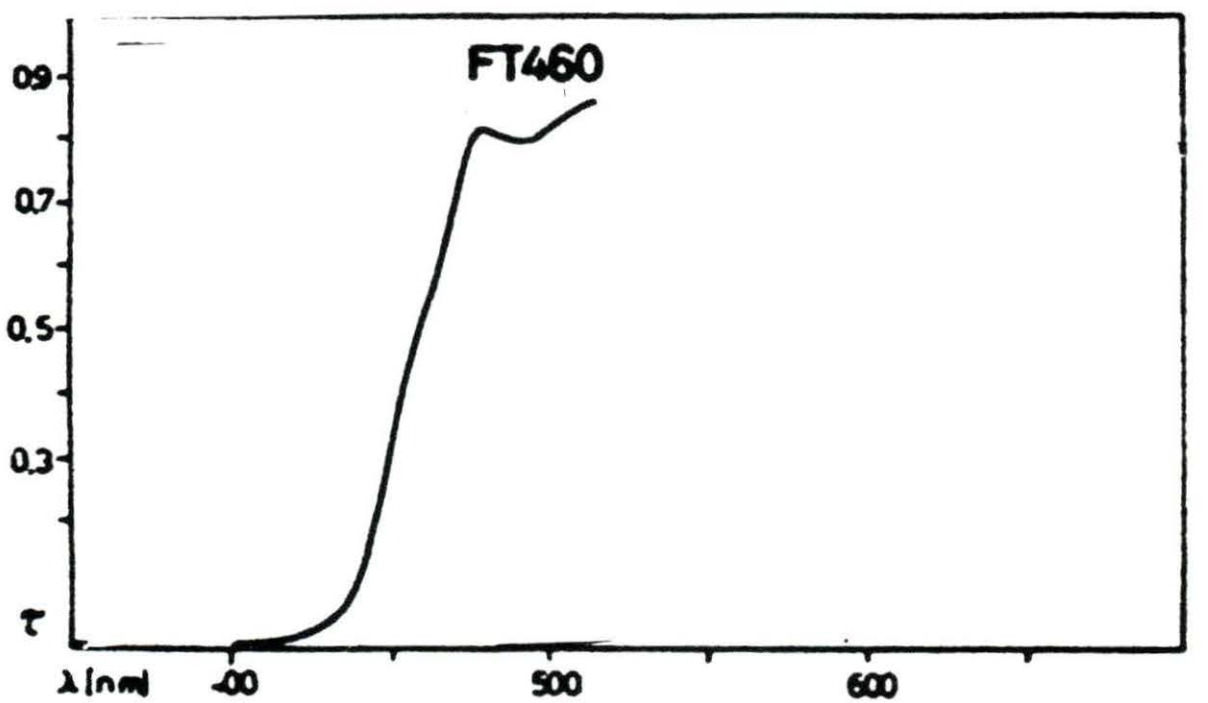

FIGURE 4.8. The transmission curve of a 460 nm dichroic beam splitter (FT 460)

From Zeiss filter specification catalog

CHAPTER FIVE: SUMMARY OF CURRENT RESEARCH

The purpose of this study was to determine if an image analysis system could be used to monitor changes in intracellular calcium concentration in individual canine blood platelets activated with the agonist ADP. Fura-2 (a fluorescent calcium-detecting dye), a Zeiss Axiophot fluorescence microscope, a silicon intensified target (SIT) camera, and a digital image processing system were used.

Fura-2-loaded platelets were obtained by following conventional procedures outlined in the literature. Although a temperature controlled cell chamber was designed and implemented to maintain the platelets at 37 °C and to allow administration of the agonist ADP, microscopy was done at room temperature because of focusing problems. The cells were excited at 340 nm and 380 nm exciting radiation produced by a 50-W Hg high pressure vapor burner.

Epi-fluorescence, a scheme whereby exciting radiation as well as emitted fluorescence pass through the microscope objective to and from the specimen, was achieved by using a 395 nm dichroic mirror. The emitted fluorescence passed through the dichroic mirror and a 420 nm long pass barrier filter before striking an ultrasensitive SIT camera. The SIT camera was used to

obtain video fluorescence images of the Fura-2-loaded platelets. The output of the camera was digitized to a resolution 480 x 512 pixels by the digital image processing unit with each point in the image being assigned a grey value from 0 to 255, depending on intensity. Each of three samples of platelets was excited at 380 nm and then at 340 nm and their fluorescence images were recorded. Ratio operations ($R_{340/380}$) were performed for each pair and recorded.

The following results and conclusions were presented:

- Fluorescence images at 380 nm exciting radiations were more intense than those at 340 nm, and the ratio image ($R_{340/380}$) indicated that calcium-free dye concentration was greater than that of the calcium-bound dye. The results possibly indicated that $[Ca^{2+}]_i$ was at the basal level, which would then have indicated that platelets were not activated. It could be argued that Fura-2/AM was not hydrolyzed in the cells to the calcium-sensitive Fura-2 because of insufficient equilibration time. However, Sample Three platelets was equilibrated for at least two hours at 37 °C before being examined under the microscope. The results from the fluorescence images at 340 nm and 380 nm exciting radiation and the ratio ($R_{340/380}$) were consistent with those from Sample One and Sample Two which were equilibrated for 15 minutes and one hour,

respectively. It is, therefore, unlikely that Fura-2/AM remained largely esterified.

- The fluorescence intensity of platelet images varied from one platelet to another, and it was concluded that Fura-2/AM did not load uniformly into platelets.
- Fura-2/AM did not load into platelets from hemolyzed blood. This was possibly due to dye hydrolysis by esterases released from damaged red blood cells.
- Comparison between images obtained from Fura-2-loaded platelets without ADP and the same images with ADP showed no changes, a result which indicated that platelets were not responsive to ADP. This was attributed to possibilities such as temperature, loss of sensitivity to ADP, low fluorescence intensity at 340 nm, or the absence of extracellular calcium in the bathing medium.

The following conclusions concern the uv excitation source, the SIT camera, and the behavior of Fura-2/AM over time.

- The 50-W Hg lamp had a low output intensity at 340 nm. Since various optical components in the optical path of the exciting beam have relatively poor transmission characteristics at 340 nm, it was concluded that this source was not adequate for excitation at 340 nm.
- The SIT camera, with its high sensitivity, low level intensity requirement, and large dynamic range, was an

essential component for obtaining fluorescence images. The vision field of the SIT camera was smaller than that of the microscope objective. However, this limitation did not pose a problem in this series of experiments.

* The fluorescence and loading abilities of Fura-2/AM in buffered solution and used over a period of four weeks, at the end of a three-month storage period frozen in DMSO, seemed to decrease as a function of time. Aliquots of Fura-2/AM dissolved and subsequently frozen in DMSO appeared to be stable over a three-month period.

CHAPTER SIX: RECOMMENDATIONS FOR FUTURE RESEARCH

Detection of changes in $[Ca^{2+}]_i$ in individual platelets using fluorescence microscopy with dual excitation wavelengths and digital image processing is a feasible method. The following are recommendations for continuing the current line of research: areas such as corrections for dark current and spatial variations in the SIT camera gain, the uv excitation source, background fluorescence correction, signal-to-noise ratio increase, data collection, and Fura-2 fluorescence enhancement in platelets.

The SIT Camera

It has been established that the SIT camera is an essential and critical component in the image processing system. There are, however, corrections that need to be made regarding spatial variations in camera dark current and gain.

- Spatial variations in dark current can be reduced by obtaining averaged images without input to the camera and then subtracting them from fluorescence images on a pixel-per-pixel basis [Williams et al., 1985].
- Spatial variations in camera gain and source excitation intensity can be reduced by multiplying images by a "system normalization map". This map is obtained by

recording the fluorescence image of a well-mixed Fura-2 free acid solution and then dividing each point in the field by the mean fluorescence intensity [Williams et al., 1985].

UV Excitation Source

It has been determined that the 50-W Hg vapor burner is not an adequate source for fluorescence ratio imaging because of the low output intensity at 340 nm exciting radiation. Therefore, either a 100-W Hg lamp (as was used by Connor et al. [1987]), or a Xenon lamp, with its higher intensity output at 340 nm, both with an optical density filter associated with the 380 nm excitation, is a more suitable uv source.

Infrared Blocking

Parts of the spectral output of a typical mercury vapor burner lie in the infrared region. Since it is possible that some infrared radiation could be reflected toward the SIT camera, it is recommended that an infrared-blocking filter be placed before it.

Background Fluorescence

Correction for background fluorescence of cells and other objects such as dust and debris, excited with uv

radiation in the absence of Fura-2, can be made by obtaining a baseline value at both 340 nm and 380 nm and then subtracting that value from the Fura-2 fluorescent images.

Signal-to-Noise Ratio

The enhanced images obtained at 340 nm were "noisy" because of the very low fluorescence intensity level. The signal-to-noise ratio can be increased by sequentially adding multiple frames to memory and/or by increasing the excitation source intensity.

Data Collection

Valuable information can be extracted from studying fluorescence images of platelets over time. This can be done by taking several frames of fluorescence images at both excitation wavelengths over time intervals and then studying their respective ratios. This process can be repeated for activated platelets to determine the time dependence of dye-bleaching and changes in $[Ca^{2+}]_i$. Time studies can also be applied to platelets under prolonged incubations in HEPES buffered solution with 1 mM $[Ca^{2+}]_o$.

Approximate quantitative measurements can be realized with the image processing system by establishing grey value curves for known calcium concentrations in solutions

containing Fura-2 pentapotassium salt and an environment similar to the intracellular milieu. Then, comparisons can be made between the grey values obtained for unknown $[Ca^{2+}]_i$ and those curves.

Fluorescence Enhancement

Fluorescence intensity can be increased by using freshly prepared Fura-2/AM in buffered solution and by increasing the concentration of the dye from 4 μM to 10 μM as reported by Tsien et al. [1985]. However, increasing dye-concentration also increases perturbation of cell functions. More experiments should be conducted to determine a Fura-2/AM concentration which enhances fluorescence and also minimally interferes with cell functions.

BIBLIOGRAPHY

Almers, W., and E. Neher. 1985. The Ca signal from fura-2 loaded mast cells depends strongly on the method of dye-loading. F.E.B.S. Letters 192(1):13-18.

Al-Mohanna, Futwan A., and Maurice B. Hallett. 1988. The use of fura-2 to determine the relationship between cytoplasmic free Ca^{2+} and oxidase activation in rat neutrophils. Cell Calcium 9:17-26.

Ashley, C. C., L. M. Castell, C. Osborn, K. Pritchard, and A. E. G. Raine. 1985. Applications of fluorescent Ca^{2+} indicators for the measurement of cytoplasmic free Ca^{2+} concentrations in platelets and lymphocytes. J. Physiol. (London) 369:23P.

Blinks, John R., and Edwin D. W. Moore. 1986. Practical aspects of the use of photoproteins as biological calcium indicators. Pages 229-238 in Paul De Weer and Brian M. Salzberg, eds. Optical methods in cell physiology. Volume 40. Society of General Physiologists Series and Wiley-Interscience, New York, New York.

Blinks, John R., W. Gil Wier, Peter Hess, and Franklyn G. Prendergast. 1982. Measurement of Ca^{2+} concentrations in living cells. Prog. Biophys. Molec. Biol. 40:1-114.

Bush, Douglas S., and Russell L. Jones. 1987. Measurement of cytoplasmic calcium in aleurone protoplasts using Indo-1 and Fura-2. Cell Calcium 8:455-472.

Campbell, A. K., T. J. Lea, and C. C. Ashley. 1979. Coelenterate photoproteins. Pages 13-72 in Christopher C. Ashley and Anthony K. Campbell, eds. Detection and measurement of free Ca^{2+} in cells. Elsevier/North-Holland, New York, New York.

Clemmons, R. M., and K. M. Meyers. 1984. Acquisition and aggregation of canine blood platelets: Basic mechanisms of function and differences because of breed origin. Am. J. Vet. Res. 45(1):137-144.

Cohen, Lawrence B., and Sarah Lesher. 1986. Optical monitoring of membrane potential: Methods of multisite optical measurement. Pages 71-99 in Paul De Weer and Brian M. Salzberg, eds. Optical methods in cell physiology. Volume 40. Society of General Physiologists Series and Wiley-Interscience, New York, New York.

Connor, John A., Hsiu-Yu Tseng, and Philip E. Hockberger. 1987. Depolorization and transmitter-induced changes in intracellular Ca^{2+} of rat cerebellar granule cells in explant cultures. J. Neuroscience 7(5):1384-1400.

Fay, Fredric S., Kevin E. Fogarty, and James M. Coggins. 1986. Analysis of molecular distribution in single cells using a digital imaging microscope. Pages 51-63 in Paul De Weer and Brian M. Salzberg, eds. Optical methods in cell physiology. Volume 40. Society of General Physiologists Series and Wiley Interscience, New York, New York.

Feinstein, M. B. 1980. Release of intracellular membrane-bound calcium precedes the onset of stimulus-induced exocytosis in platelets. Biochem. Biophys. Res. Commun. 93(2):593-600.

Feinstein, Maurice B., George B. Zavoico, and Stephen P. Halenda. 1985. Calcium and cyclic AMP: Antagonistic modulators of platelet function. Pages 237-269 in Gesina L. Longenecker, ed. The platelets: Physiology and pharmacology. Academic Press, Inc., Orlando, Florida.

Fukuo, Keisuke, Shigeto Morimoto, Eio Koh, Shiro Yukawa, Hiroyasu Tsuchiya, Shunji Imanaka, Hideki Yamamoto, Toshio Onishi, and Yuichi Kumahara. 1986. Effects of prostaglandins on the cytosolic free calcium concentration in vascular smooth muscle cells. Biochem. Biophys. Res. Commun. 136(1):247-252.

Ganong, W. F. 1987. Review of medical physiology. Appleton & Lange, San Mateo, California.

Gray, Peter, ed. 1973. The encyclopedia of microscopy and microtechnique. Van Nostrand Reinhold Company, New York, New York.

Grynkiewicz, Grzegorz, Martin Poenie, and Roger Y. Tsien. 1985. A new generation of Ca^{2+} indicators with greatly improved fluorescence properties. J. Biol. Chem. 260(6):3440-3450.

Hallam, Trevor J., and Timothy J. Rink. 1985. Responses to adenosine diphosphate in human platelets loaded with the fluorescent calcium indicator quin2. J. Physiol. (London) 368:131-146.

Hallam, Trevor J., Ana Sanchez, and Timothy J. Rink. 1984. Stimulus-response coupling in human platelets: Changes evoked by platelet-activating factor in cytoplasmic free calcium monitored with the fluorescent calcium indicator quin2. Biochem. J. 218:819-827.

Hallam, T. J., M. Poenie, and R. Y. Tsien. 1986. Homogeneity of ADP- and thrombin-stimulated rises in $[Ca^{2+}]_i$ in fura2-loaded human platelet populations revealed by fluorescence ratio image processing. J. Physiol. (London) 377:123p.

Jain, N. C. 1986. The platelets: Structural, biochemical, and functional aspects. Pages 446-465 in Schlam's veterinary hematology. Lea & Febiger, Philadelphia, Pennsylvania.

Jones, Harold P. 1985. Calmodulin and platelet function. Pages 221-235 in Gesina L. Longenecker, ed. The platelets: Physiology and pharmacology. Academic Press, Inc., Orlando, Florida.

Le Breton, G. C., R. J. Dinerstein, L. J. Roth, and H. Feinberg. 1976. Direct evidence for intracellular divalent cation redistribution associated with platelet shape change. Biochem. Biophys. Res. Commun. 71(1):362-370.

Luckhoff, Andreas. 1986. Measuring cytosolic free calcium concentration in endothelial cells with Indo-1: The pitfall of using the ratio of two fluorescence intensities recorded at different wavelenghts. Cell Calcium 7:233-248.

Matthews, J. A. 1987. The effects of age and aspirin on porcine platelet function. Ph.D. Thesis. Iowa State University.

Meyers, Kenneth M. 1985. Pathobiology of animal platelets. Advances in Veterinary Science and Comparative Medicine 30:131-165.

Moran, David T., and J. Carter Rowley. 1987. Biological specimen preparation for correlative light and electron microscopy. Pages 1-22 in M. A. Hayat, ed. Correlative microscopy in biology: Instrumentation and methods. Academic Press, Inc., Orlando, Florida.

Nemeth, E. F., Jean Wallace, and Antonio Scarpa. 1986. Stimulus-secretion coupling in bovine parathyroid cells: Dissociation between secretion and net changes in cytosolic Ca^{2+}. J. Biol. Chem. 261(6):2668-2674.

Pollock, W. K., and T. J. Rink. 1986. Thrombin and ionomycin can raise platelet cytosolic Ca^{2+} to micromolar levels by discharge of internal Ca^{2+} stores: Studies using fura-2. Biochem. Biophys. Res. Commun. 139(1):308-314.

Pollock, Kenneth W., Timothy J. Rink, and Robin F. Irvine. 1986. Liberation of [^{3}H] arachidonic acid and changes in cytosolic free calcium in fura-2-loaded human platelets stimulated by ionomycin and collagen. Biochemical J. 235:869-877.

Pritchard, K., and C. C. Ashley. 1986. Na^+/Ca^{2+} exchange in isolated smooth muscle cells demonstrated by the fluorescent calcium indicator fura-2. F.E.B.S. Letters (1,2) 195:23-27.

Rao, Gundu H. R., E. Radha, and James G. White. 1983. Effect of docosahexaenoic acid (DHA) on arachidonic acid metabolism and platelet function. Biochem. Biophys. Res. Commun. 117(2):549-555.

Rao, Gundu H. R., Janet D. Peller, and James G. White. 1985. Measurement of ionized calcium in blood platelets with a new generation calcium indicator. Biochem. Biophys. Res. Commun. 132(2):652-657.

Reynolds, G. T. and D. L. Taylor. 1980. Image intensification applied to light microscopy. BioScience 30(9):586-592.

Rink, Timothy J., and Tullio Pozzan. 1985. Using Quin2 in cell suspensions. Cell Calcium 6:133-144.

Rink, T. J., S. W. Smith, and R. Y. Tsien. 1982. Cytoplasmic free Ca^{2+} in human platelets: Ca^{2+} thresholds and Ca-independent activation for shape-change and secretion. F.E.B.S. Letters 148(1): 21-26.

Sage, S. O. , and T. J. Rink. 1986. Kinetic differences between thrombin-induced and ADP-induced calcium influx and release from internal stores in fura-2-loaded human platelets. Biochem. Biophys. Res. Commun. 136(3):1124-1129.

Scarpa, A. 1979. Measurement of calcium ion concentrations with metallochromic indicators. Pages 85-115 in Christopher C. Ashley and Anthony K. Campbell, eds. Detection and measurement of free Ca^{2+} in cells. Elsevier/North-Holand, New York, New York.

Shipman, Charles, Jr. 1969. Evaluation of 4-(2-Hydroxyethyl)-1-Piperazineethanesulfonic Acid (HEPES) as a Tissue Culture Buffer. Proceedings of the Society of Experimental Biology and Medicine. 130:305-310.

Tank, David W., Mutsuyuki Sugimori, John A. Connor, and Rodolfo R. Llinas. 1988. Spatially resolved calcium dynamics of mammalian Purkinje cells in cerebellar slice. Science 242:773-777.

Tsien, Roger Y. 1980. New calcium indicators and buffers with high selectivity against magnesium and protons: Design, synthesis, and properties of prototype structures. Biochemistry 19:2396-2404.

Tsien, R. Y. 1981. A non-disruptive technique for loading calcium buffers and indicators into cells. Nature. 290:527-528.

Tsien, Roger Y. 1983. Intracellular measurements of ion activities. Ann. Rev. Biophys. Bioeng. 12:91-116.

Tsien, Roger Y. 1986. New tetracarboxylate chelators for fluorescence measurement and photochemical manipulation of cytosolic free calcium concentrations. Pages 327-345 in Paul De Weer and Brian M. Salzberg, eds. Optical methods in cell physiology. Volume 40. Society of General Physiologists Series and Wiley Interscience, New York, New York.

Tsien, R. Y., T. Pozzan, and T. J. Rink. 1982. Calcium homeostasis in intact lymphocytes: Cytoplasmic free calcium monitored with a new, intracellularly trapped fluorescent indicator. J. Cell Biol. 94:325-334.

Tsien, R. Y., T. Pozzan, and T. J. Rink. 1984. Measuring and manipulating cytosolic Ca^{2+} with trapped indicators. Trends in Biochemical Sciences 9:263-266.

Tsien, R. Y., T. J. Rink, and M. Poenie. 1985. Measurement of cytosolic free Ca^{2+} individual small cells using fluorescence microscopy with dual excitation wavelengths. Cell Calcium 6:145-157.

Waggoner, Alan S. 1986. Fluorescent probes for analysis of cell structure, function, and health by flow and imaging cytometry. Pages 3-28 in D. Lansing Taylor, Alan S. Waggoner, Robert F. Murphy, Fredrick Lanni, and Robert R. Birge, eds. Applications of fluorescence in the biomedical sciences. Alan R. Liss, Inc., New York, New York.

White, James G., and Jonathan M. Gerrard. 1978. Platelet morphology and the ultrastructure of regulatory mechanisms involved in platelet activation. Pages 17-34 in Giovanni de Gaetano and Silvio Garattini, eds. Platelets: A multidisciplinary approach. Raven Press, New York, New York.

Williams, David A., Kevin E. Fogarty, Roger Y. Tsien, and Fredric S. Fay. 1985. Calcium gradients in single smooth muscle cells revealed by the digital imaging microscope using Fura-2. Nature 318:558-561.

Wolf, Paul L., Patricia Ferguson, Irma Torquati Mills, Elisabeth Von der Muehll, and Mary Thompson. 1973. Practical clinical hematology: Interpretations and techniques. John Wiley & Sons, New York, New York.

Yardumian, D. A., I. J. Mackie, S. J. Machin. 1986. Laboratory investigation of platelet function: A review of methodology. J. Clin. Pathol. 39:701-712.

ACKNOWLEDGEMENTS

I would like to express my deepest appreciation to Dr. W. H. Brockman and Dr. Mary Helen Greer. They have both provided me with tremendous support, advice, and constructive criticism. They guided me through this long and challenging journey and kept me afloat until I completed this project. My appreciation is extended to Dr. Philip Haydon for his willingness to serve on my POS committee. He was also very generous with his time and provided me with helpful techniques on handling Fura-2/AM.

Many thanks are directed toward Dr. Carol Jacobson, Cristy Larracey, and Steve Vanderwiel for their generous time, patience, and assistance with the digital image analysis equipment.

I would like to thank Dr. Arlo Ledet and the veterinary pathology lab technicians for allowing me to use the Wright stain machine and for giving me more information about platelets.

This project would not have been possible without Laboratory Animal Resources. I would like to thank Dr. Joan Hopper and Felice Iasevoli for letting me use lab dogs for my research. Week after week Deb, Burt, and Dean extracted blood from dogs for my research.

This work is dedicated to my parents, Souad and Nabhan, who have endured tremendous hardships to support

me both financially and emotionally. My brothers, Majdi and Ammar, have been with me every step of the way; I especially appreciate Majdi's support and guidance.

The typing of this manuscript has been a product of the expert and critical work of Chris Diesch. My thanks are also extended to Dr. Kurt Diesch who generously allowed me the use of his computer. The completion of this thesis was made ever so interesting by their newborn, Elizabeth Anne Diesch (June 12, 1989).

I would like to thank the Madduxes: Jere, Linda, Drew, and KTG for being like a family to me. A special thank you goes to Linda for editing my thesis.

The stress related to this work has been eased by the love and support of Brenda Harms and her wonderful family.

I appreciate the support of the BME faculty and students.

I would like to thank Mrs. LaDena Bishop for her expert editing of this manuscript.

May all Palestinians live peacefully in their homeland and may the world live in peace.

APPENDIX

This section consists of Figure A.1 through Figure A.6. These figures are those of the unenhanced fluorescence images collected by the methods described in Chapters Three and Four. It is noted that the images are distorted in intensity and that further enhancement was necessary to obtain visually interpretable data.

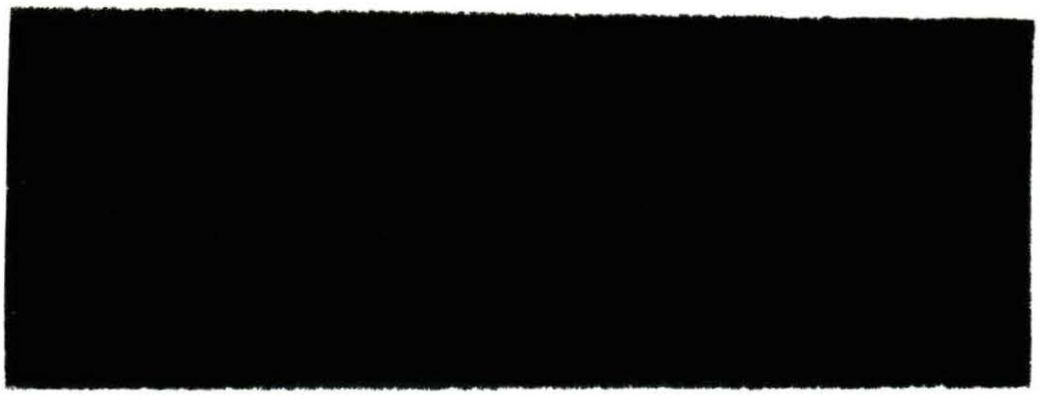

(a)

(b)

FIGURE A.1. Unenhanced fluorescence image of Sample ONE platelets due to excitation at:

a) 380 nm exciting radiation

b) 340 nm exciting radiation

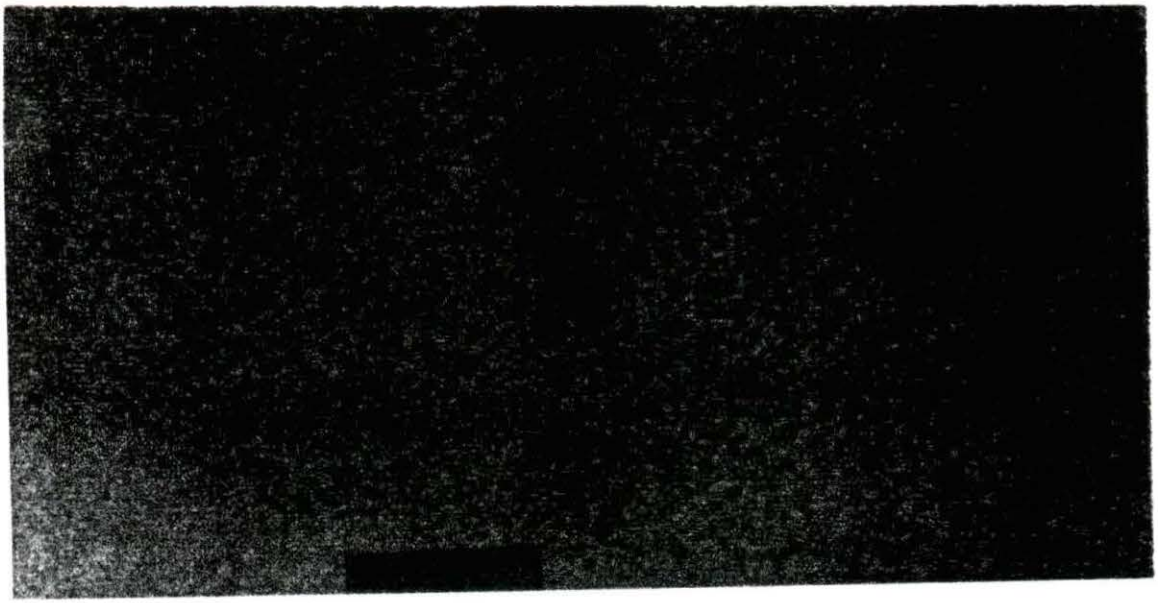

FIGURE A.2. Unenhanced ratio image ($R_{340/380}$) of Sample ONE platelets

The fluorescence image due to 340 nm excitation radiation was divided by that due to 380 nm excitation on a pixel-per-pixel basis

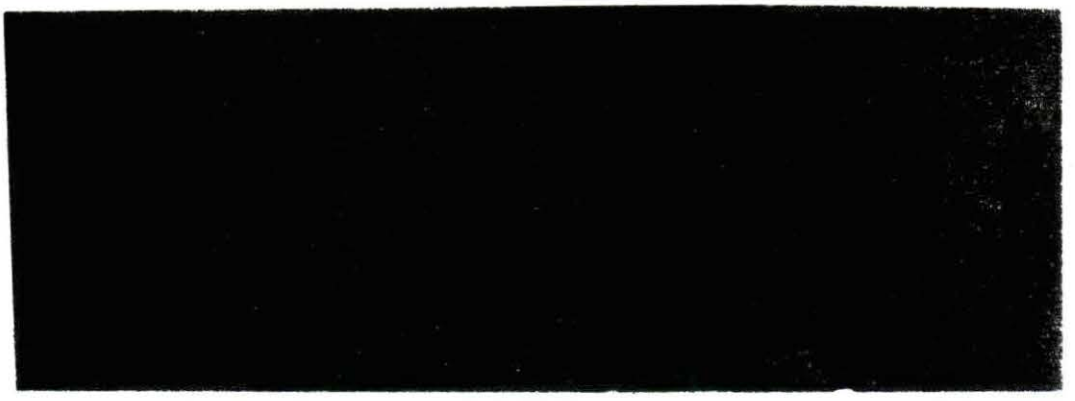

(a)

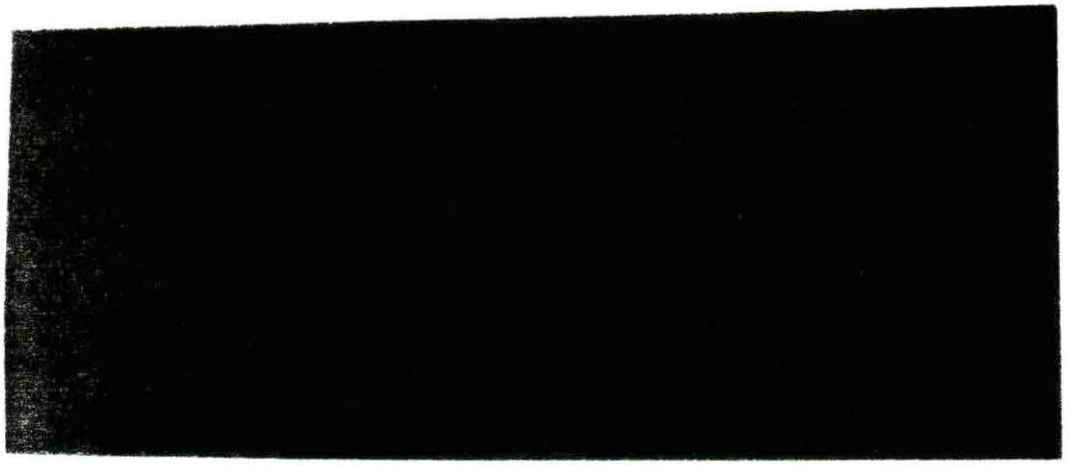

(b)

FIGURE A.3. Unenhanced fluorescence image of Sample TWO platelets due to excitation at:

a) 380 nm exciting radiation

b) 340 nm exciting radiation

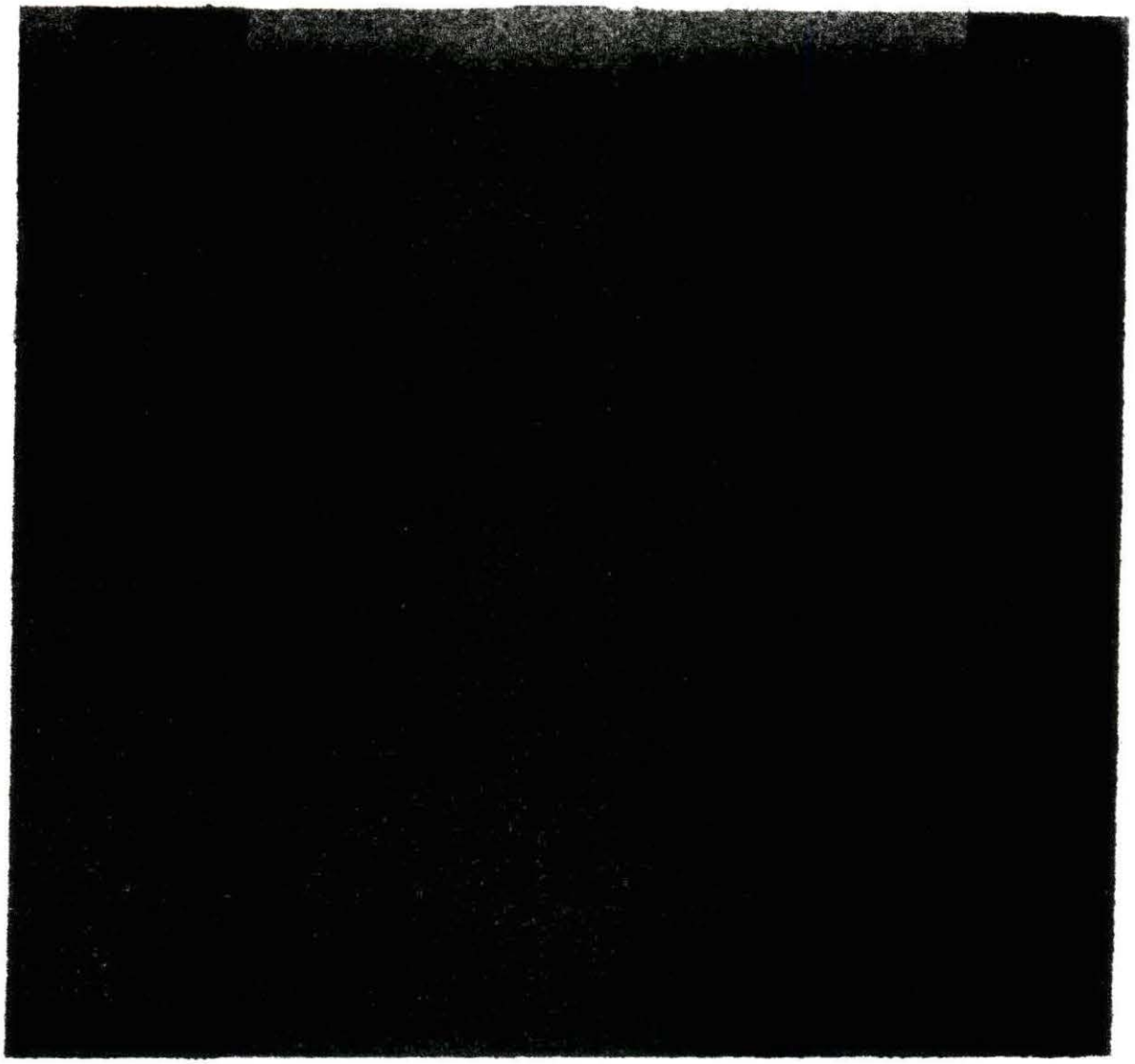

FIGURE A.4. Unenhanced ratio image ($R_{340/380}$) of Sample TWO platelets

The fluorescence image due to 340 nm excitation was divided by that due to 380 nm excitation on a pixel-per-pixel basis

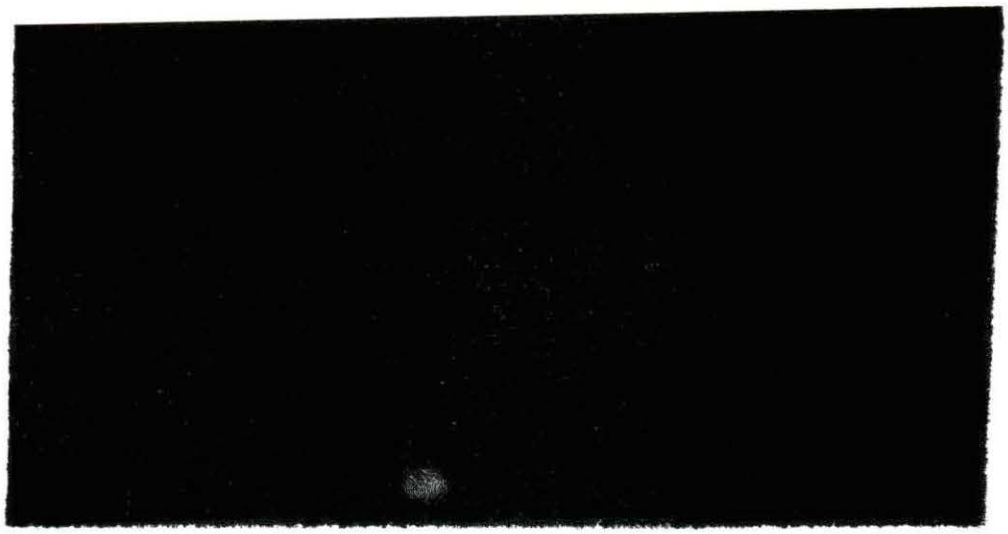

(a)

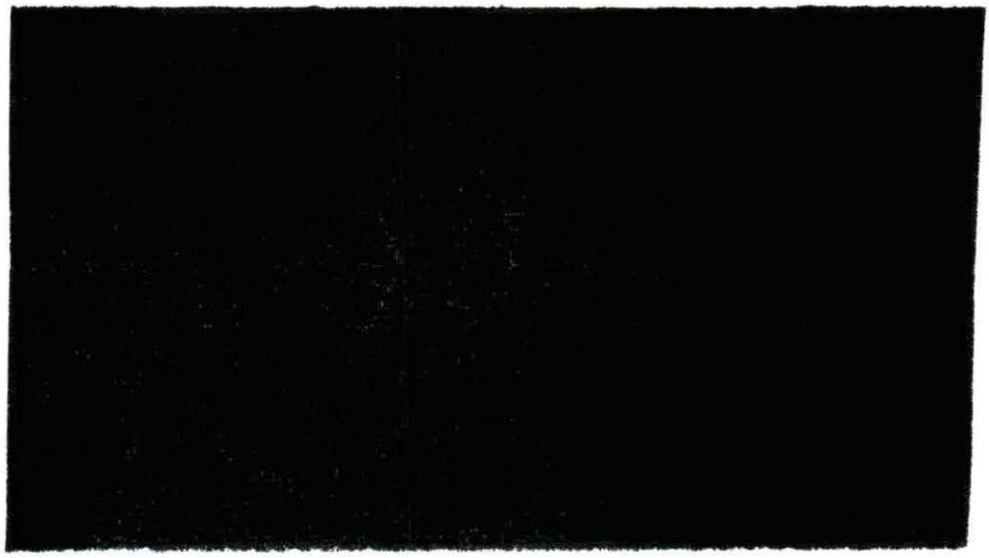

(b)

FIGURE A.5. Unenhanced fluorescence image of Sample THREE platelets due to excitation at:

a) 380 nm exciting radiation

b) 340 nm exciting radiation

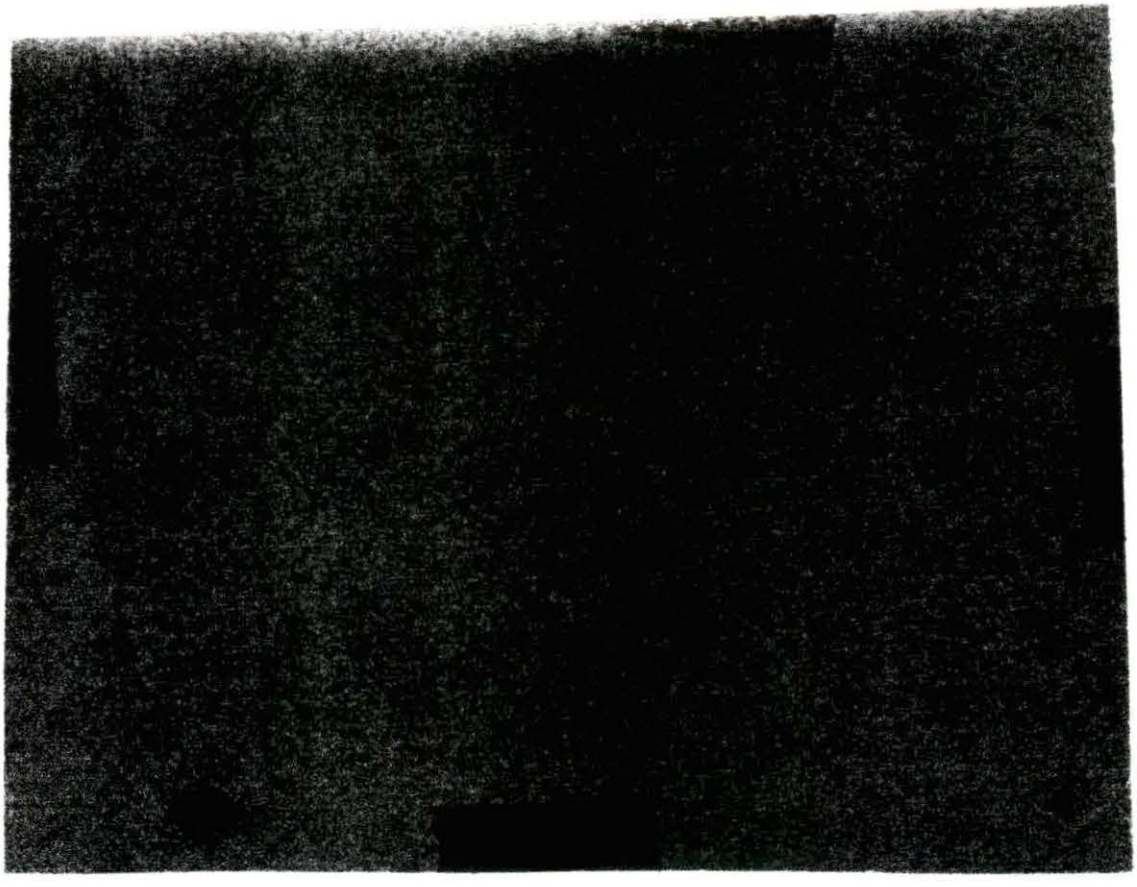

FIGURE A.6. Unenhanced ratio image ($R_{340/380}$) of Sample THREE platelets

The fluorescence image due to 340 nm excitation was divided by that due to 380 nm excitation on a pixel-per-pixel basis